ORIGINAL PAPER

Shear Behaviour of Fibreglass Rock Bolts for Various Pretension Loads

Peter Gregor[1] · Ali Mirzaghorbanali[1,2] · Kevin McDougall[3] · Naj Aziz[4] · Behshad Jodeiri Shokri[1,2]

Abstract

In this paper, after determining an appropriate experimental design and testing scheme to test the shear performance suitably, the impacts of pretension and shear interfaces on fibreglass rock bolts were investigated. For this purpose, at the first stage, the double shear testing apparatus was modified to address the issues and shortcomings of the established testing methodology. Then, 20-tonne and 30-tonne rock bolts were tested with pretension loads of 0 kN, 10 kN, 15 kN, and 20 kN for each test scheme. For this, a 40 MPa small aggregate concrete was used for all samples to simulate the host rock. The grout used to anchor the rock bolts was mixed to the product's recommended guidelines to ensure close resemblance to field mixtures. To maintain consistency, all samples were manufactured with the same concrete and grout recipes. The results of double shear tests revealed that increasing the pretension also increased the confining pressures at the shear interfaces for clean joints. This, in turn, reduced the damage propagating from the bolt at the shear interface and decreased the hinge point bending. The results can be applied for further analytical and numerical studies, which could utilise for a better understanding of the shear behaviour of fibreglass rock bolts.

Highlights

- Two types of fibreglass rock bolts, the 20-tonne and 30-tonne rock bolts, were tested utilising the modified double-shear apparatus.
- The double-shear testing apparatus was modified to address the issues and shortcomings of the established testing methodology.
- The double shear performance profiles of the bolts could be described by three regions categorised as the elastic, strain-softening, and failure regions.
- Increasing the pretension of each rock bolt type resulted in a reduction in the severity of the recorded shear force dip.
- The increased pretension yielded less physical damage to the rock bolt propagating away from the shear plane.

✉ Behshad Jodeiri Shokri
Behshad.JodeiriShokri@usq.edu.au

1   School of Engineering, University of Southern Queensland, Springfield Campus, Springfield, QLD 4300, Australia

2   Centre for Future Materials (CFM), University of Southern Queensland, Toowoomba, QLD 4350, Australia

3   School of Surveying and Built Environment, University of Southern Queensland, Toowoomba Campus, Toowoomba, QLD 4350, Australia

4   School of Civil, Mining & Environmental Engineering, University of Wollongong, Wollongong, NSW 2500, Australia

1 Introduction

The mining industry is one of the largest industries in Australia. According to the Reserve Bank of Australia, the mining industry has seen a dramatic increase in its industry share from the fifth position at 6.3% in 2016 to 11.1% in 2020, placing it as the second largest industry in Australia (Reserve Bank of Australia 2020). With the current growth of the mining sector, there is a need to prevent the increase in fatalities. Therefore, the employer must provide a safe work environment, especially underground spaces. A safer

work environment can be achieved through better design and understanding of environmental factors, such as failure mechanisms and conditions contributing to instability. One such way failure conditions, and instability can be minimised is the correct installation of tendons. Tendons are highly efficient and cost-effective technology that can be implemented as primary or secondary support systems. Primary support systems, usually rock bolts, which are a part of the active reinforcements, are installed during excavation and aim to maintain or increase the strength properties of the rock mass. Secondary support systems, such as cable bolts, supplement the primary supports and can be implemented by either a passive or active method (Windsor 1997).

There are a wide variety of rock bolt designs such as torque tension bolt fibreglass, injection bolts GFRP, S20/200GFRP, S22/250GFRP, S25/350GFRP, AH Solid Bar Steel, AROA GFRP, MB1F32G Fibreglass, MB1F-32GRT Fibreglass, and FBM Steel, which are available in the Australian market, including mechanically anchored, fully encapsulated, cuttable, and friction lock to name a few (Li 2017a; MINOVA 2021; Jennmar 2021; DSI-UNDERGROUND 2021; MEGA-BOLT 2021). Unlike steel, fibreglass rock bolts combine two primary elements; linearly aligned glass fibres and thermo-set resin (Frketic et al. 2017). As such, the resultant rock bolt is comprised of a uniaxial structure that results in anisotropic performance (Maranan et al. 2015), in stark contrast to the isotropic matrix of metallic rock bolts. The study conducted by Aziz et al. (2015b) investigated the difference between isotropic and anisotropic rock bolts. It concluded that axially loaded fibreglass rock bolts could achieve up to 85% of the ultimate tensile strength of steel. However, when loading the sample perpendicular to the fibre direction (i.e., shear loading), the rock bolt's shear failure load averaged only 25% of the metallic rock bolt. The low shear performance of fibreglass rock bolts has limited their use to rib reinforcements where limited shearing is present (Li et al. 2016). Despite reduced performance limits to that of metallic rock bolts, fibreglass rock bolts possess significant benefits over their metal counterparts: including cutability and corrosion resistance. During coal extraction, rib supports are often removed with the advancement of shearers. Therefore, fibreglass rock bolts are often chosen over metallic rock bolts as the shearer heads can safely cut the fibreglass rock bolts without inflicting damage during the extraction (Gilbert et al. 2015). Additionally, studies conducted by Hassell et al. (2004), Spearing et al. (2010), and Aziz et al. (2013) outlined the detrimental effects of corrosion on metallic rock bolts and their susceptibility to such environments. Aziz et al. (2013) outlined the four critical forms of corrosion impacting steel: uniform, localised, mechanically assisted, and environmentally assisted degradation. Due to the non-metallic nature of fibreglass rock bolts, they demonstrate improved resistance

to corrosive environments. As a result, fibreglass rock bolts are commonly implemented as supports in highly corrosive environments such as coal mines.

For many years, axial load transfer mechanism, shear load mechanism, single shear testing, and double shearing tests were utilised for investigating the mechanical behaviour of rock bolts, such as axial bearing capacity and shearing properties (Chang et al. 2017; Clifford et al. 2001; Forbes et al. 2020; Hartman 2003; Jahangir et al. 2021; Rajapakse 2016; Li et al. 2017b; Mirzaghorbanali et al. 2017; Thenevin et al. 2017; Thompson et al. 2014; Waclawik et al. 2019; Windsor et al. 1992). The shearing performances of rock bolts can be determined using a few methods, each with a varying representation of the bolts in situ conditions. Shearing tests developed include the single shear guillotine test in accordance with the British Standard for testing (BS 7861 2009), the double shear guillotine test, and concrete embedded double shear testing (DST) (Gilbert et al. 2015). Single shear testing (SST) is accomplished by cutting the tendon along a single plane. Three testing systems have since been developed and are still in use today, including the British Standard (BS 7861 2009) single shear test (BSST), direct single shear, and the Megabolt single shear tests (Aziz et al. 2017). Each test evaluates different aspects of the tendon's performance. For instance, the direct single shear test applies the shear load directly to the bolt with no incorporated buffer and, as such, identifies the pure shear property for the bolt, while the BSST method aims at testing the performance of bolts in strata. Due to the presence of strata bedding, multiple shear planes can be induced on a single bolting system (Nemcik et al. 2006). As a result, the DST method was developed to simulate the actual field conditions. The DST apparatus consists of a single bolt grouted into three concrete blocks, as first developed by Aziz et al. (2003). DST methodology was designed with three types: MKI, MKII, and MKIII (Aziz et al. 2016). MKIII is the modified version of MKII and both are used for the shear strength determination of high strength tendons such as cable bolts. The double shear box is comparable to the Megabolt shear test as it incorporated simulated concrete strata to replicate the effects of localised crushing (Aziz et al. 2015a).

The double shear box was initially used to investigate varying host strata UCS. The study conducted by Gilbert et al. (2015) using the MK1 double shear apparatus provided an understanding of the relationship between shear strength and host UCS by subjecting rock bolts to host rock strengths of 40 MPa and 60 MPa. As a result, the study observed two unique and increasing ultimate shear failure loads and concluded that the shear performance of rock bolts was a function of the host rock UCS. Gilbert et al. (2015) used the MK1 double shear testing apparatus from the Aziz et al.'s (2003) study to also compare the shear load transfer mechanisms of fibreglass rock bolts using the single shear testing

method (i.e., Guillotine box). A limited number of tests were carried out on fibreglass rock bolts using the double shear testing method (MKI). When compared to the single shear test method, it was concluded that (a) single shear testing of guillotine box underestimates the shear strength of fibreglass rock bolts; (b) shear strength of fibreglass rock bolts is a function of pretension values, and (c) strata strength (i.e., concrete strength) affects the shear strength of fibreglass rock bolts. Furthermore, Li et al. (2016) identified the mechanism whereby the weaker host rock crumbles at the shearing plane allowing the rock bolt to flex inducing additional stresses on the rock bolt element. Samples tested at 60 MPa were identified as less susceptible to this phenomenon and indicated that an increase in the host rock UCS resulted in an increase in the overall shear performance of the rock bolts. The MK1 double shear box was further modified to allow for the investigation of varying bolt pretensions. The study conducted by Aziz et al. (2015b) adopted the MK1 double shearing apparatus to investigate the effect of pretension on the shear performance of rock bolts. Pretension values of 2.5, 5, 10, and 15 kN were chosen for the study. Despite the non-uniform distribution of pretension values, the study highlighted an increase in the ultimate shear failure in the presence of pretension. MKI is the suggested testing method for non-metallic rock bolts, such as fibreglass bolts, as per Aziz et al. (2015b).

The literature review revealed that few of the identified research investigated fully grouted fibreglass rock bolts of various tensile strength capacities as per the manufacturer's design, installed with various pretension settings, and subjected to shearing. There were also limited studies investigating the impact of shear interface types on various tensile rated fibreglass rock bolts' shear performance. Therefore, the main objectives of this research are (a) determining an appropriate experimental design and testing scheme to suitably test the shear performance of fibreglass rock bolts and (b) undertaking a comprehensive experimental study to determine the shear strength of two fibreglass bolts under varying pretension values for clean joint interfaces. Indeed, this research will answer the following questions: (a) How does the application of pretension affect the shear load transfer mechanism and final shear performance of fibreglass rock bolts? (b) What impact do various tensile strengths of fibreglass rock bolts have on the shear performance of fibreglass rock bolts with clean shear interfaces?

2 Materials and Methods

2.1 Experimental Plan for Clean Discontinuities

Testing was conducted on several fibreglass rock bolts with commonly used tensile load capacity ratings of 20 and 30 tonnes. Double shear testing was conducted by investigating

Table 1 Experimental matrix for effect of pretension

Dowel (tonne)	Strata (MPa)	Pretensions (kN)
20	40	0
		10
		15
		20
30	40	0
		10
		15
		20

Fig. 1 Outline of SANS Machine used for double shear testing

the effect of bolt strength on the shear performance of fibreglass rock bolts at a range of pretension values. Fibreglass rock bolts of various strengths were tested to determine the rock bolts' performance on a passive rock bolt system (i.e., no pretension). The results formed the baseline performance data of rock bolts for a simplified uniform environment. The strata UCS value was chosen following the study conducted by Li et al. (2016). This study identified the host strata UCSs of 20 MPa, 40 MPa, and 60 MPa as accurate representations of field conditions. The 40 MPa concrete strength was then chosen for casting simplicity. Additionally, wet concrete at a target strength of 40 MPa was found to have ideal workability. The weaker 20 MPa and stronger 60 MPa mixtures were either too wet or too stiff to handle efficiently. The second experimental study explored the effects of varying pretension values on the shear strength of fibreglass rock bolts. A single host media strength of 40 MPa was used to maximise sample uniformity. The fibreglass bolts were fastened using their respective nuts and washers and torqued to pretension values of 0%, 5%, 10%, and 15% of each rock
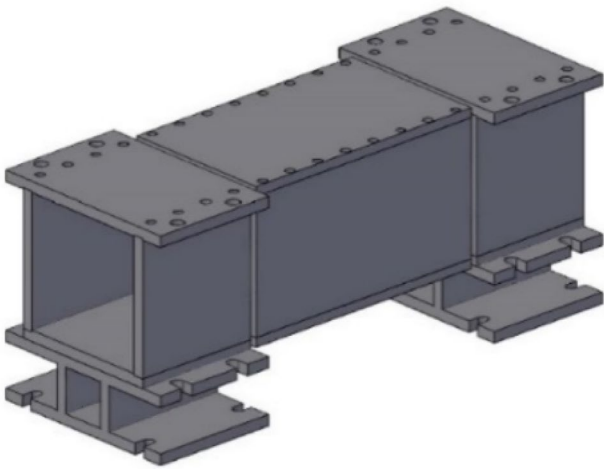
Fig. 2 MK1.5 Double shear box design

bolt's maximum tensile load capacity with industry standards as indicated by Gilbert et al. (2015). The prepared samples were then sheared at the rate of 1 mm/min (Gilbert et al. 2015). Table 1 outlines the experimental plan that was followed to successfully conduct the in-depth analysis of the mechanical properties of fibreglass dowels used to reinforce

clean joints. A total of eight tests were conducted for the completion of the clean discontinuity investigation.

2.2 Equipment Design

Double shear testing was carried out using the 150-tonne compression-testing machine at the University of Southern Queensland Engineering Laboratory. The prepared samples were positioned inside the testing machine and then subjected to shearing at the shearing rate of 1 mm/min (Gilbert et al. 2015). The shear displacement was exerted on top of the middle block by a levelling load plate, and the shear load was measured using a calibrated load cell as highlighted in Fig. 1. The load cell was attached directly to the shearing plate, and the data were collected using an inbuilt data acquisition system.

2.3 Shear Box

To provide confinement around the concrete block during shear testing, a steel shear box shown in Fig. 2 was designed and manufactured according to the samples' dimensions and as per the shear testing procedure (Li et al. 2016). The confinement impeded premature failure of the concrete blocks during shear testing, allowing fibreglass to achieve

Fig. 3 Assemble double shear apparatus highlighting key features such 10 mm spacing at each interface
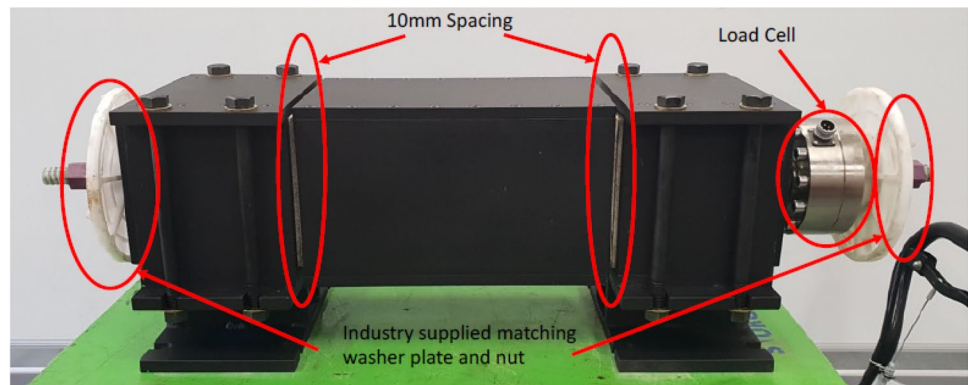
**Fig. 4** Centre block rotation because of testing
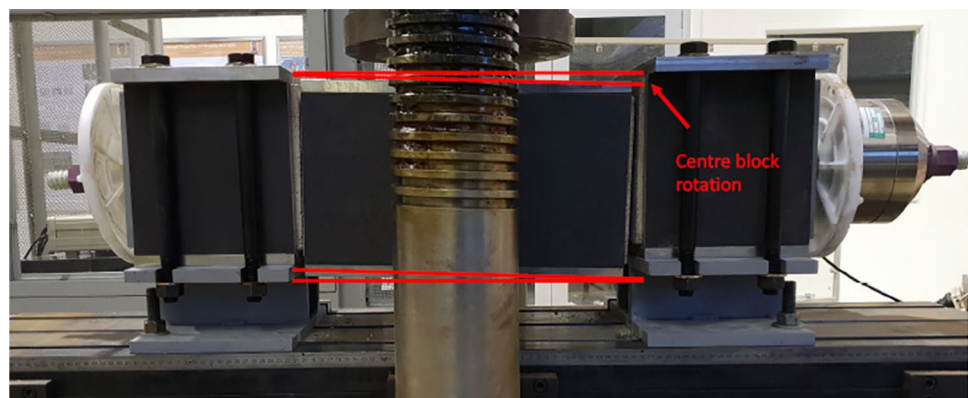
its maximum shear strength capabilities. In civil and mining field conditions, confinement is provided naturally via surrounding strata.

The overall length of the confining box was 780 mm, with the total concrete length being 800 mm. The 20 mm difference in length created a 10 mm allowance for the shearing planes. It was essential to minimise the unencapsulated surface area and maintain symmetry as the exposed area encounters different confinement pressures and has the potential to cause premature concrete failure

around the jointed section. As such, the 20 mm spacing was applied 5 mm to each side of the shearing plane, as illustrated in Fig. 3.

The 5 mm spacing on each side of the shearing plane successfully addressed the issues relating to frame wedging by the British standards testing method, as depicted in Fig. 3. Despite the British standard of testing measuring single shear performance, the rotation encountered during testing was also present during double shear testing, as shown in Fig. 4. It is noted that the addition of the

Fig. 5 a Double shear mould key features; **b** preparation for rifling simulation

(a) **(b)**
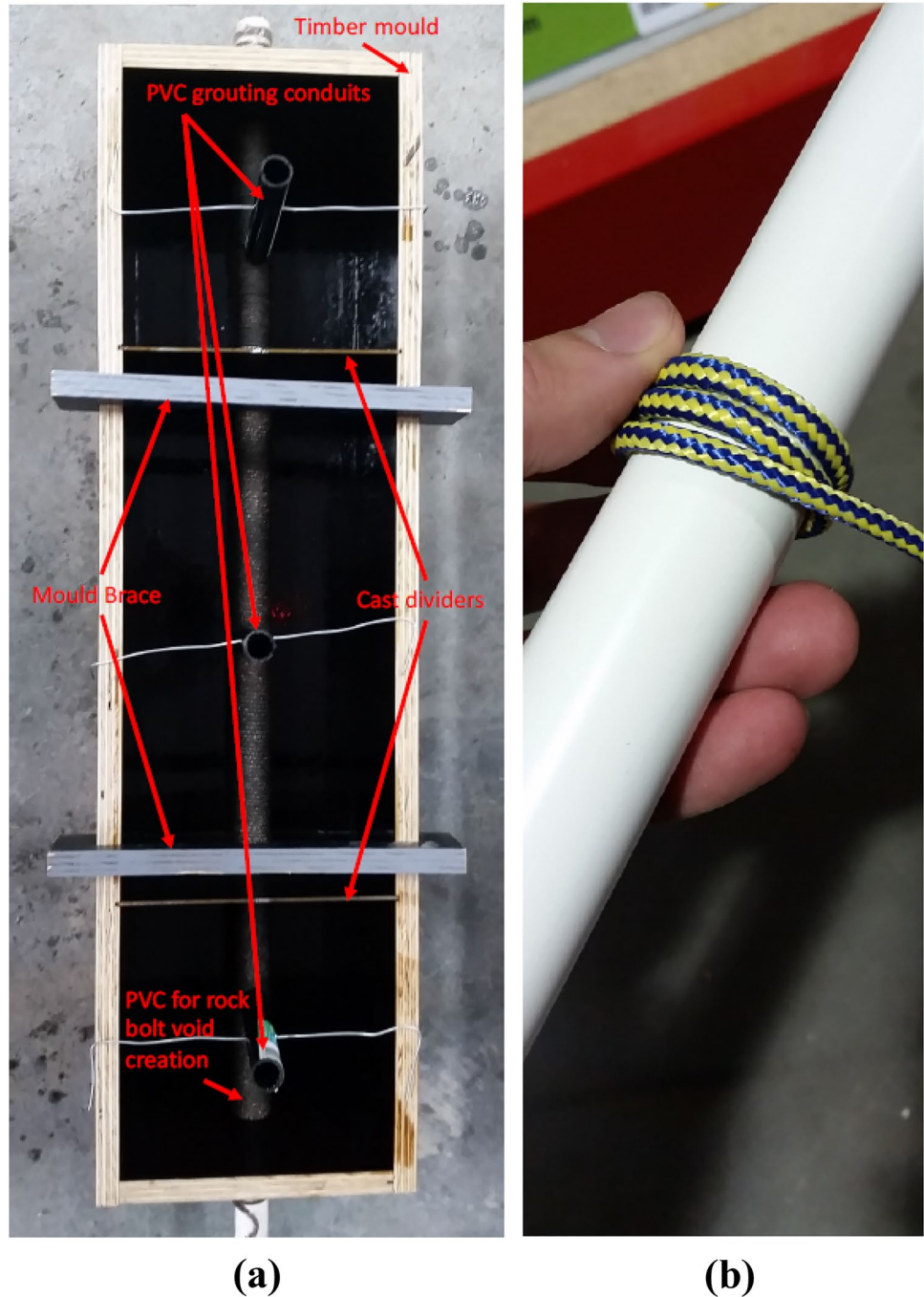
5 mm spacer was successful with no evidence of frame wedging. While this method does not remove the presence of shear rotation, it successfully minimises the potential of mechanical interference of the test frame at the shear planes.

2.4 Mould Design

Moulds were constructed utilising the UniSQ workshop CNC facilities to ensure uniform casting parameters. Each mould was designed to produce three concrete blocks that were later assembled to form a system with two shear planes. The blocks of the outer edge of the double shear system were cast to the dimensions of 200 mm by 200 mm by 200 mm and the centre block to the dimensions of 200 mm by 200 mm by 400 mm with a longitudinally intersecting hole with a radius of 16 mm.

The mould consisted of timber panels, metal dividers, braces, and an intersecting PVC pipe, as shown in Fig. 5a. The braces were used to minimise mould deformation under the weight of the concrete during curing. A rope was wrapped around the PVC pipe to create a cavity for the rock bolt and simulate the rifling that results from the drilling process; a rope was wrapped around the PVC pipe, as illustrated in Fig. 5b. However, care was taken to wrap the rope sparingly as the initial attempts resulted in the rope exerting inward axial forces on the pipe, increasing the difficulty of disassembly. Once the concrete was poured and levelled, PVC conduits were then inserted into the centre of each block intersecting the PVC pipe. The conduits create a small channel directly to the rock bolt location allowing for a more straightforward grout charging process. Finally, excess concrete was poured into 100 mm diameter by 200 mm steel moulds for future UCS testing.

2.5 Sample Preparation

As per the experimental plan, the concrete blocks were cast to 40 MPa specifications using a mortar recipe following the guidelines from Gilbert et al. (2015). Two concrete

Fig. 6 Severe damage resulting from a weak concrete matrix

specifications were cast, the first designed to achieve a UCS of 20 MPa and the second to achieve 40 MPa. Initially, the low-strength 20 MPa sample was cast using the cement, sand, and water ratio of 1:3:0.7, successfully resulting in consistency like that of sandstone. Coarse sand was used instead of aggregate to maintain cross-sectional uniformity. By adopting a low-strength mortar-based recipe, the initial testing of samples proved that the mixture did not have sufficient strength to shear the rock bolt. Figure 6 shows the severe damage the concrete blocks sustained before achieving failure within the rock bolt element. Therefore, the mixture was adjusted to achieve a minimum strength of 40 MPa using a cement, sand, and water ratio of 1:2.2:0.42.

Fig. 7 Cylindrical concrete samples for UCS testing

Table 2 UCS test results of the concrete used for double shear casting

Sample	Pressure (MPa)	Load (kN)
1	29.10	228.7
1.3	52.65	413.3
2	50.50	396.6
3	55.90	438.8
4	50.90	400.0
6	59.40	466.8
7.1	83.76	657.5
7.2	61.50	482.9
8	78.85	619.0
9	67.50	529.7
Average	47.81	375.48

The concrete production was completed using the climate-controlled facilities and curing room at the University of Southern Queensland to maintain consistency and high-test quality. Each concrete batch was mixed using the onsite concrete mixer and set into the moulds using a vibrator and scraper to remove bubbles and impurities, resulting in clean, uniform samples. The concrete was left to set for 24 h, after which the moulds were disassembled, and the blocks were placed into the curing room for a minimum of 28 days.

Samples were capped using plaster of Paris to minimise the impact of stress concentrations forming from surface imperfections because of casting. The fine composition of the plaster fills the surface irregularities and facilitates the optimum transfer of forces. Before testing the double shear blocks, the cylinders of the corresponding batch were tested under compression conditions to determine the actual host UCS (Fig. 7). The UCS results are presented in Table 2 and indicate an average of 48 MPa. All samples tested met the minimum strength requirements, and as a result, all double shear tests were successfully performed to achieve rock bolt failure prior to host medium failure.

2.6 Pre-tensioning

Once the concrete samples were cured, the fibreglass bolts were positioned into the precast holes for final assembly. The rock bolt, concrete blocks, axial load cell, and washer plates were assembled loosely and in the correct order for final tightening, as illustrated in Fig. 8. The pretension was then applied to the desired value per the experimental plan in Table 3. The pretension (kN) was determined using a

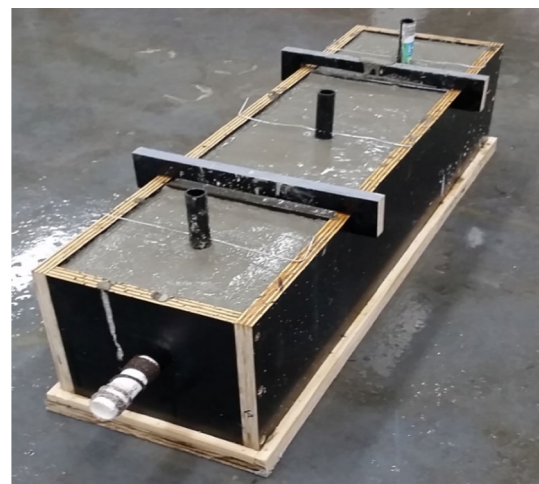**Fig. 8** Assembly of the double shear samples

Fig. 9 Concrete casting mould used to manufacture the blocks of the double shear system

Table 3 Properties for 20-tonne and 30-tonne tensile rated rock bolts subjected to the clean shear test system

Bolt type	Rock bolt diameter (mm)	Rock bolt length (mm)	Design shear capacity (t)	Designed pre-tension (kN)	Tested pre-tension (kN)	Rate of loading (mm/min)
20 T0 kN C	20	1200	20	0	1	1
20 T10 kN C	20	1200	20	10	12.8	1
20 T15 kN C	20	1200	20	15	13.5	1
20 T20 kN C	20	1200	20	20	20.5	1
30 T0 kN C	20	1200	30	0	0.8	1
30 T10 kN C	20	1200	30	10	11	1
30 T15 kN C	20	1200	30	15	12	1
30 T20 kN C	20	1200	30	20	17.5	1

Fig. 10 Grouting quality examination after testing

Fig. 11 Initial unconfined test 30-tonne

previously installed hollow load cell to monitor axial loads. The pretension value varied between 0 and 20 kN, similar to those currently applied in Civil and Coal Mining industries (Gilbert et al. 2015). The minimum pretension value of 0 kN was achieved by installing wedges in the edge of the holes to overcome the weight forces of the washers, rock bolts, and load cells, and ensure the system was centred. The remaining pretensioned samples had sufficient axial loads to ensure the system was centred. To minimise the effects of creep and

settling, all samples had their respective pretensions applied 24 h before grouting.

2.7 Grouting

In the last stage of sample preparation, the reinforced concrete blocks were grouted through holes on top of the sample, as shown in Fig. 9.

Once the samples were cast and grouted, any excess grout was removed from the injection holes and cleaned smoothly to prevent stress concentrations. The sheared samples were then dismantled to investigate the grout encapsulation quality. As demonstrated in Fig. 10, the rock bolt was appropriately centred within the bore, and the grout successfully encapsulated the entirety of the bolt with minimal voids. The highlighted section of Fig. 10 illustrates the microridges formed by the rope technique adopted in Sect. 2.4. The adopted techniques allowed for uniform encapsulation throughout all samples' annulus areas. Samples were left for additional 7 days to allow the grout/fibreglass interface to strengthen and ensure that the grout strength exceeded that of the concrete.

2.8 Initial Testing

2.8.1 Unconfined Shear Samples

Two preliminary double shear tests were carried out on reinforced concrete blocks without confinement. The test results were undertaken to trial the success and efficiency of the preparation method adopted. Tests were performed on 20 MPa and 40 MPa concrete blocks reinforced with 30-tonne fibreglass rock bolts with no confining pressure as seen in Fig. 11. Bolts were set to passive mode (i.e., no pretension) and sheared at a 1 (mm/min) shearing rate.

After 1 day of curing, the prepared sample was positioned in the compression-testing machine. The peak shear load values were 5.7 and 8.5 tonnes for 20 and 40 MPa concrete blocks, respectively. Due to samples being tested in an unconfined environment, the rock bolts did not achieve

Fig. 12 High-quality encapsulation (left) around fibre glass bolt (right) around the concrete medium

failure, and the test became an analysis of the system bending performance. Samples were carefully dismantled after testing to investigate the quality of grouting and encapsulation, as shown in Fig. 12. High-quality encapsulations were observed for both the fibreglass bolt and concrete medium.
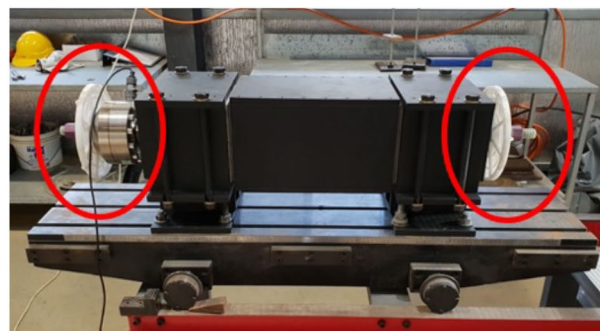
2.8.2 Confined Shear Samples

The main double shear tests were carried out on reinforced concrete blocks using the MK1.5 designed confinement shear box, as shown in Fig. 3. Tests were performed on 20 MPa concrete blocks reinforced with 30-tonne fibreglass bolts. The bolt was set with a pretension of 10 kN and sheared at 1 mm/min shearing rate. The first test conducted using the pretension of 10 kN. It is evident that there is a significant axial transfer of load resulting in the pretension doubling to 22 kN. Additionally, confined samples have also achieved a greater shear load to that of the preliminary study.

2.9 Fibreglass Rock Bolt

The GRP bolts selected for this study were supplied by Applied Research of Australia (AROA) and were manufactured using the pultrusion method. The bolts selected for testing included the 20-tonne dowel and the 30-tonne dowel. Due to the unconventional testing method adopted throughout the double shear stage of this study, custom samples were required: both in length and thread design. Figure 13 (top) indicates that the typical bolt design includes threads at only one end of the dowel, as the other end remains embedded in the strata. However, the modified double shear testing equipment requires both ends of the dowel to remain exposed to allow for symmetry of the system and the application of pretension; this can be seen in Fig. 13 (bottom).

2.9.1 Double Shear Calculations

The results of the double shear tests were analysed and reduced to both material properties and overall system performance. Each test output was reported as force and displacement represented by kilonewtons and millimetres. Furthermore, the shear force data represented the overall double shear force, and therefore, Eq. (1) reduces the data to represent the forces exerted on each plane.

$$F_{\text{Shear Plane}} = \frac{F_{\text{Double Shear}}}{2}, \tag{1}$$

where $F_{\text{Double Shear}}$ is the raw test data in Newtons (N); $F_{\text{Shear plane}}$ is the forces isolated to the failed shear plane in Newtons (N).

Additionally, the recorded results did not outline the stresses experienced by the rock bolts at the peak shear loads. Therefore, Eq. (2) was used to calculate the peak shear stress and results in a value with the units of gigapascals

$$\tau_{\text{Stress}} = \frac{F_{\text{Shear plane}}}{\pi r^2}; \tag{2}$$

$F_{\text{Shear Plane}}$ is the forces isolated to the failed shear plane in Newtons (N); τ_{Stress} is the ratio between shear force and cross-sectional area in (N/m^2); r is the nominal rock bolt radius in metres (m).

3 Results and Discussion

3.1 Overview of the Testing Process

As discussed earlier, the testing was conducted on fibreglass rock bolts commonly used by the industry with design

Fig. 13 (Top) illustration of fibreglass bolt geometry; (bottom) double shear testing apparatus with double-ended threads

tensile load capacity ratings of 20 and 30 tonnes. As a result, the double shear tests were used to identify and compare the peak strength of 20-tonne and 30-tonne dowels in a simulated multi-shear plane environment with clean shear interfaces. For this purpose, samples were prepared to utilise a host media strength of 40 MPa to simulate moderate-strength rock conditions. Then, the fibreglass bolts were fastened using their respective nuts and washers. Smooth shear interfaces were achieved during the casting process by utilising metal plates. Samples were then torqued to pretension values of 0 kN, 10 kN, 15 kN, and 20 kN.

Table 3 outlines the rock bolts' properties and their designed pretension forces when subject to the clean shear interface test programme. Also highlighted in Table 3 are the physical design characteristics of the selected bolts along with their designed pretension, achieved pretension, and rate of loading.

It is noted that there were variations to the achieved pretension values due to the rock bolts' settling during curing. Unfortunately, this element could not be controlled, and some rock bolts experienced more settling than others. To minimise the variation of settled pretensions, several steps were implemented. First, corrections were made during the initial hour of the grout's curing process until the grout was sufficiently set. After the initial setting stage, any additional adjustments would have a limited impact on the internal pretension of the system. The initially applied pretension was set to 3 kN greater than the designed limit to minimise pretension variation. Unfortunately, each sample varied, and some experienced more significant reductions in pretension, resulting in values less than the target pretension. In contrast, other samples exhibited reduced settling rates and achieved values slightly greater than the target pretension.

3.2 Results for 20-Tonne Rock Bolts, Double Shear Testing

3.2.1 Shear Behaviour Profile

The 20-tonne rock bolts were installed in the simulation system with applied pretensions of 0 kN, 10 kN, 15 kN, and 20 kN and then tested as part of a clean shear environment. Shear loads were applied to the centre of the sample using a compression-testing machine. The shear force and displacement data were simultaneously measured by internal load cells and subsequently recorded in the data logger.

Each 20-tonne sample exhibited similar shear load profiles consisting of three stages: elastic, strain-softening, and failure, as highlighted in Fig. 14a. Figure 14b illustrates how the sample subjected to 20 kN pretension displayed an approximate 2° decrease in gradient when transitioning from the elastic region to the strain-softening region. When the sample transitioned into the strain-softening stage, any

further deformation could not be reversed, resulting in permanent damage to the rock bolt. This process continued until the sample reached the failure stage. The failure stage was identified by cascading internal strand failures culminating in the ultimate failure of the rock bolt. Due to the fibreglass rock bolts being comprised of many fine strands, the failure stage does not exclusively encompass the ultimate failure of the rock bolt. It begins when enough strands fail, resulting in the sample unable to withstand increasing shear forces. The rapid decrease in curve gradient characterised this, demonstrated in Fig. 14b, with the peak shear force occurring at 0°. The peak shear force represented the system's ultimate shear capacity, including rock bolt strength, shear plane friction, and induced confinement from the applied pretension. When the samples passed their peak shear force, the fibres within the bolt instantaneously broke resulting in the shear load dropping to the residual value of the system.

Analysis of the data identified a phenomenon impacting the shear force response of most samples during the transition from the elastic region to the strain-softening region. This behaviour was characterised by a distinct drop in the recorded shear force of approximately 2 kN to 5 kN when the sample reached a shear force of approximately 60 kN and was accompanied by an audible marker from within the sample. Upon completion of the sudden shear force drop, the samples recovered and successfully progressed through the subsequent stages of failure as highlighted by Fig. 14c. This shear force drop behaviour was identified as a recurring and repeatable event and, therefore, was inferred to have resulted from internal processes caused by forces dissipating throughout each component of the system. The data set representing the 0 kN pretension sample was discarded from analysis due to premature host material failure during testing.
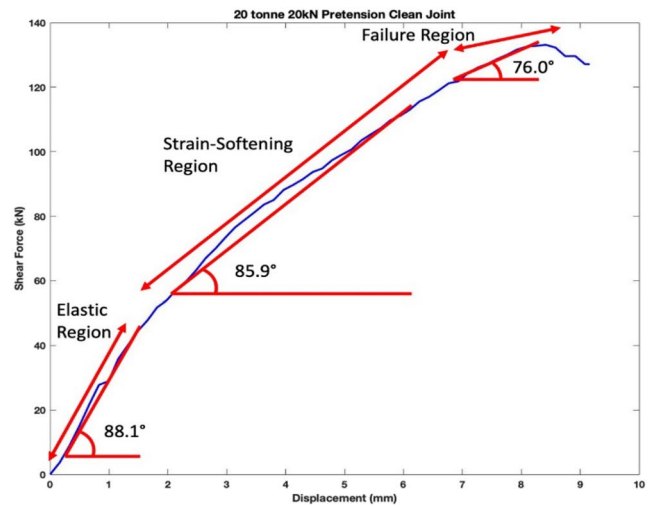
3.2.2 Pretension Profile

Figure 15a outlines that each pretension profile consisted of three stages: zone (I), zone (II), and zone III. The first zone was represented by a minor linear increase in axial force, suggesting that almost none of the applied shear force was transformed into axial force because of internal material failure. This indicated little-to-no state change between each interacting element throughout the path of shear load transformation. The graphical properties of this zone did not identify whether the rock bolt was performing in an elastic or strain failure manner. However, the shear response of zone one indicated that the components of the double shear system, such as the grout encapsulation and host material, were intact. The transition into zone (II) was defined by a significant change in gradient of approximately 3.4° when compared to zone one. Additionally, the similar displacements of zones (I) and (II) indicated that the applied shear forces
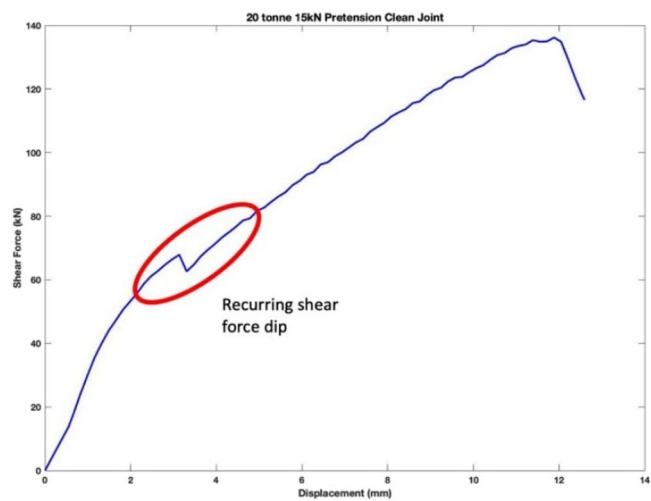
Fig. 14 **a** Example of the three failure regions for 20-tonne rock bolts; **b** change in angle for each stage of the 20-tonne double shear profile; **c** illustration of recurring reduction in shear force for 20-tonne sample
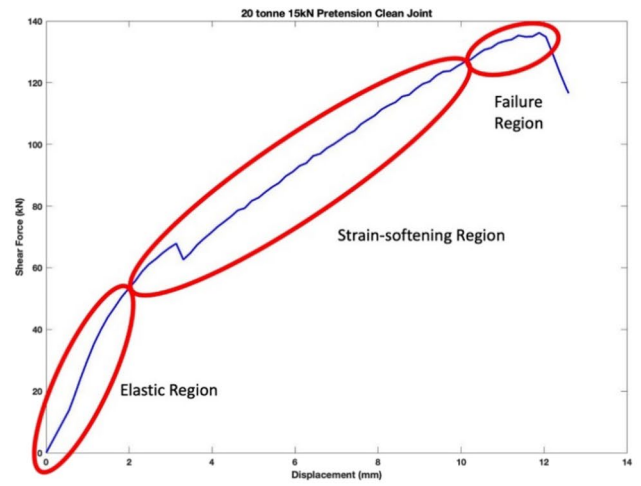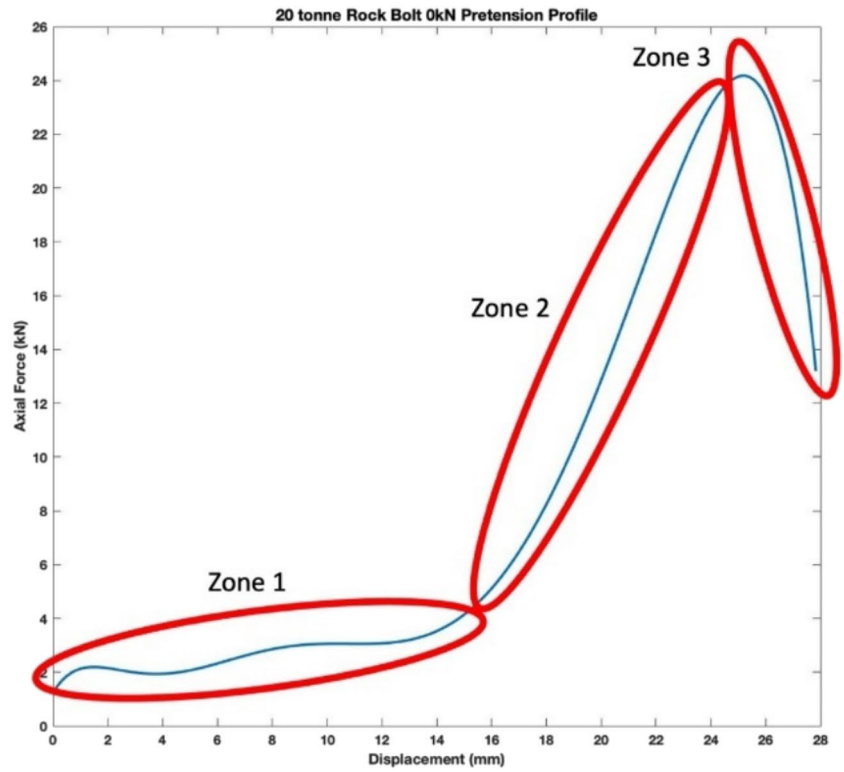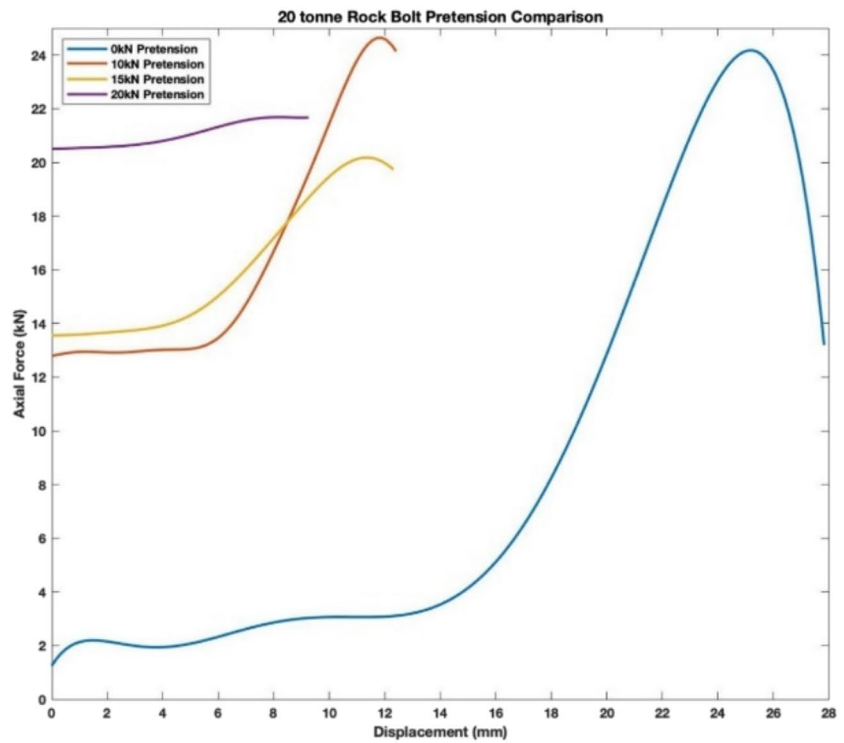

(a)

(b)

(c)

(a)

(b)

Fig. 16 a Change in shear profile due to pretension for 20-tonne rock ▶
bolts; **b** change in recorded shear dip due pretension increase from
10 to 20 kN for 20-tonne rock bolts; **c** changes to the strain-softening
stage as a result of pretension

did not transform into axial forces until approximately 50%
through the shearing process. The increase of axial forces
observed in zone two could be attributed to deteriorating
interfaces between the materials within the system, resulting
in the inability to withstand increasing loads. These failures
could have occurred between the host material and grout as
well as the grout-to-rock bolt interface. This could enable the
shear forces to transform to axial forces and transfer through
the rock bolt. Zone (III) was the final observed component
of the pretension profile, indicating the transition to total
system failure. Total system failure was identified by the
rapid drop in slope angle where increases in displacement
no longer yielded increases to the recorded axial forces. This
behaviour was a result of the fibreglass strands within the
rock bolt systematically failing until the system achieved
catastrophic failure of all strands within the rock bolt.

Several characteristics were identified when evaluating
the pretension performance of the 20-tonne rock bolts. The
increase in pretension values did not impact on the peak
axial force for samples subjected to pretension values of
10 kN and less. As a result, the 0 kN and 10 kN pretension
samples achieved peak axial forces of approximately 24 kN,
as shown in Fig. 15b. Samples subjected to pretension val-
ues of 15 kN and higher also achieved matching peak axial
forces of approximately 20 kN to 22 kN. However, these
were lower than 0 kN and 10 kN pretension samples, as
indicated in Fig. 15b. In addition to the changes in peak
axial forces, there was an observed decrease in displacement
at failure. Unlike the peak axial force's stepped response
to increased pretension, the displacement at the peak force
drastically reduced when the samples were subjected to
pretensions greater than 0 kN, suggesting a correlation
between the designed pretension and failure displacement.
The observed decrease in displacement remained constant
for each subsequent increase in pretension with an observed
displacement range of 8–12 mm as opposed to the 0 kN
pretension sample's displacement of 25 mm, as shown in
Fig. 15b. It is noted that the samples experienced force varia-
tions during curing and force settling prior to testing, result-
ing in variability from the designed pretension settings.

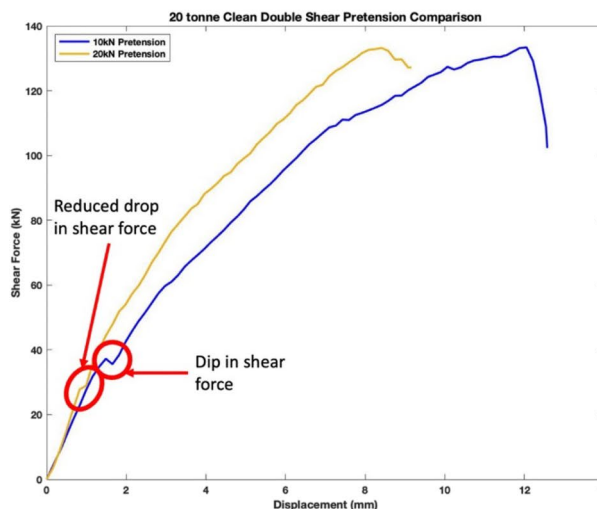### 3.2.3 Impact of Pretension on Shear Strength

Figure 16a demonstrates how the application of pretension
had no discernible impact on each sample's achieved peak
shear force. As such, each sample achieved an approximate
shear failure force of 135 kN. Additionally, samples with a
lower pretension setting did not present significant changes
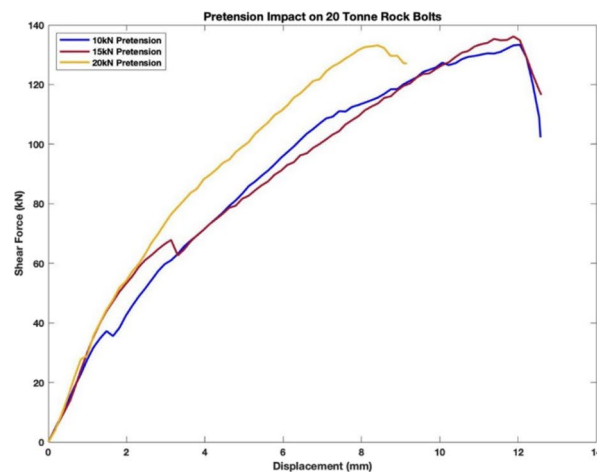
(a)
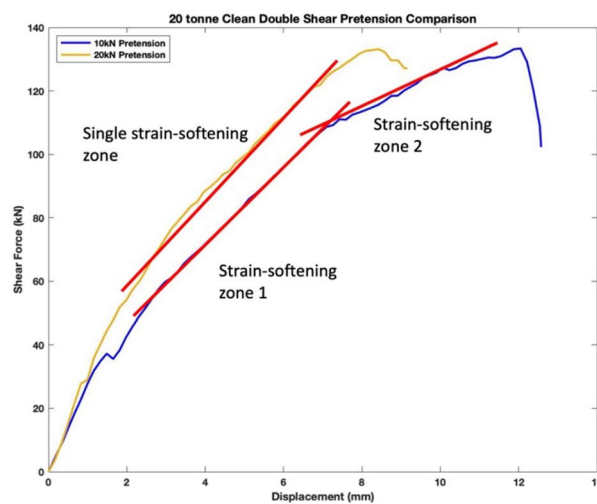
(b)

(c)

to either peak shear or displacement, as shown in Fig. 16a. Comparing the results from the 10 kN and 20 kN pretension samples, it was evident that increasing the pretension setting directly impacted on the failure displacement of the rock bolt. Figure 16a demonstrated that the failure displacement between the 10 kN and 20 kN samples reduced from approximately 12 to 8.5 mm. The change in displacement may be attributed to increased compressive forces across each shear plane because of the applied axial load imparted on the rock bolts. This force then transferred through the washer plates forcing the outer blocks together. The artificial pressures applied to the shear planes appear to have altered the confinement pressures within the grout, host rock, and their interface zones allowing them to withstand higher forces prior to failing. Increasing the confining pressures of the system facilitated a more efficient force transfer path between the loading ram and the shear planes due to less dissipation losses. As a result, a greater percentage of the applied forces were transferred to the bolt earlier in the shearing process, causing the bolt to achieve its failure limit quicker. The reduction in the dip in shear force experienced at the beginning of the strain-softening region further highlighted the significance of the altered internal pressures and is explained in Sect. 3.2.1. The sample subjected to a pretension of 20 kN exhibited a reduction in its failure displacement when compared to the 10 kN pretension sample. During shearing, the shear force halted for only approximately 0.2 mm. Figure 16b demonstrates how the 10 kN sample utilising a lower pretension experienced a shear drop of approximately 2 kN over the same region.

The increase of the pretension setting also resulted in changes to the strain-softening stage of the defined shear profile. Samples subjected to pretensions greater than 20 kN presented with a single linear representation of the rock bolts' strain-softening response to shear, highlighted in Fig. 16c. Conversely, the sample testing the impact of a 10 kN pretension shown in Fig. 16c demonstrated a strain-softening region comprised of two linear stages, with the later stage presenting with a smaller gradient. This reduction in gradient indicated the occurrence of a possible failure within the system. As previously outlined in this section, the induced system confinement due to the pretension strengthened the properties of the system materials. Therefore, it is likely that the cause of the second stage of strain-softening was due to a failure within either the grout, host material, and/or interfaces between them. Finally, the increase in pretension displayed no identifiable influence on the elastic stage of the shear profile of the tested rock bolts. It is argued that due to the samples transitioning out from the elastic region early in the shearing process, prior to the failure limits of the strata simulating materials, the elastic region was not significantly impacted by any increase in strength to defined materials.

3.2.4 Failure Characteristics

All samples were dismantled for post-failure analysis, and notable failure characteristics were highlighted. These key characteristics included the hinge point and interface damage. There was an observed correlation between the set pretension of the sample and the resultant hinge point at failure. Samples with higher pretensions recorded greater rotation at the hinge point than samples with lower pretensions. The sample set to the lower pretension of 10 kN resulted in an approximate angle of rotation of 11°. This angle increased to approximately 14° for the sample tested at 20 kN pretension, as highlighted in Fig. 17a and Table 4. The change in confinement forces due to the applied pretensions, as described in Sect. 3.2.3, is the presumed cause of the observed change in hinge point properties. The increase in the strength of the various interfaces surrounding the rock bolt caused the rock bolt to bend around the shear interface instead of pushing through and damaging the shear interface surface. The increase in the strength of the rock bolt, grout, and host rock interfaces, caused by the higher initial pretension values, resulted in less damage to the rock bolt element extending internally from the shear plane, as highlighted in Fig. 17b. Samples with a lower initial pretension value, such as the 10 kN sample, were subjected to fewer additional axial forces. The reduced axial forces resulted in a weaker shear plane and grout and host rock properties. This led to the rock bolt exhibiting a lower degree of bending at the location of failure as the surrounding material failed around the rock bolt throughout the shearing process.

Increasing the initial pretension setting exhibited no change to the damage in the vicinity of the point of shear and the surrounding material. As shown in Fig. 17c, samples prepared at both 10 kN and 20 kN pretensions, respectively, showed no signs of increased damage to the grout, simulated host rock, and shearing surface. This could be due to the limited strength of the 20-tonne rock bolts in shear resulting in the rock bolt failing prior to subjecting damage to the surrounding materials. The large fracture present in the host material displayed in Fig. 17c was a result of the processes used to split the samples post-failure to enable this analysis.

### 3.3 Results for 30-Tonne Rock Bolts, Double Shear Testing

3.3.1 Shear Behaviour Profile

The 30-tonne fibreglass rock bolts were subjected to pretensions ranging from 0 to 20 kN and clean shear joints were analysed for their response to applied shear loads. The tests were similar to the previous 20-tonne samples. After systematic tests were conducted under varying pretension conditions, the shear load profiles could be described by the
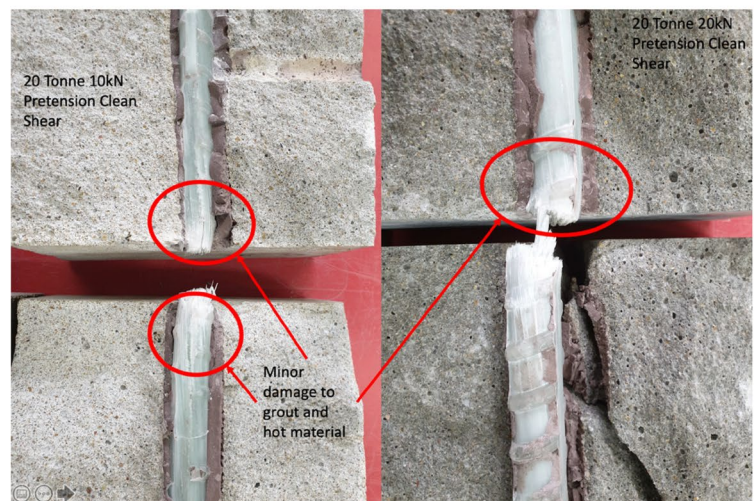
Fig. 17 **a** Angle of failure and rock bolt damage for 20-tonne 10 kN pretension clean shear rock bolt; **b** angle of failure and rock bolt damage for 20-tonne 20 kN pretension clean shear rock bolt; **c** damage caused to host material by the 20-tonne rock bolts of 10 kN and 20 kN pretensions
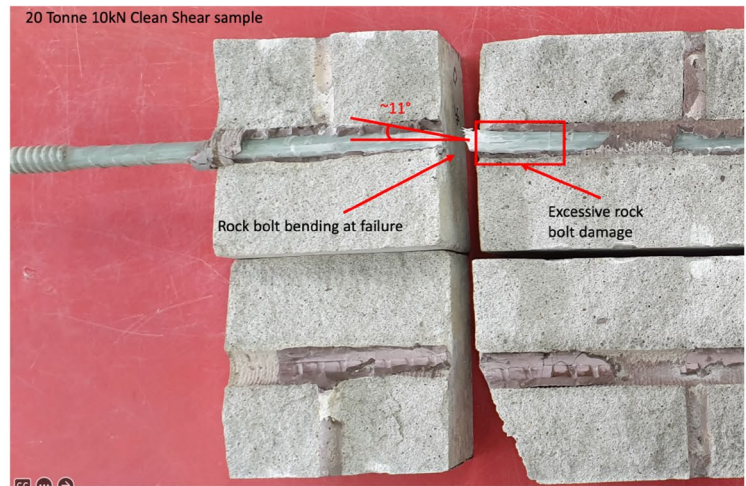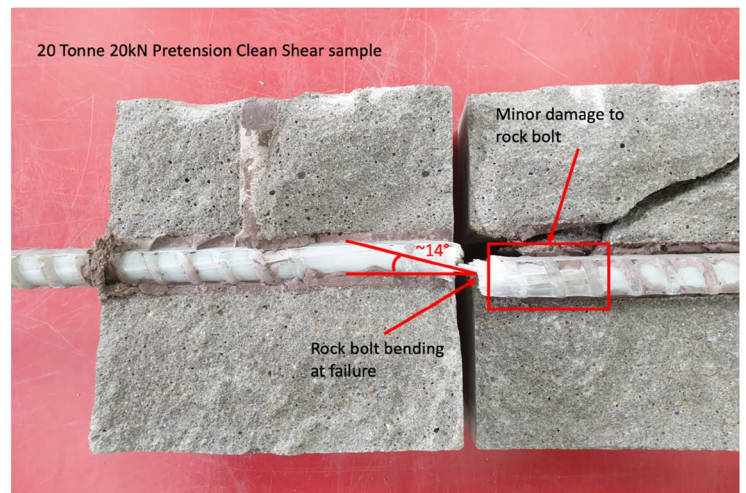
Table 4 Summary of gradients at each stage of the shear profile curve and angle at the hinge point post-failure

Rock bolt	Elastic gradient (°)	Strain softening gradient (°)	Failure gradient (°)	Angle at hinge point (°)
20 T 0 kN	Invalid	Invalid	Invalid	Invalid
20 T 10 kN	87.7	84.8	78.7	11.0
20 T 15 kN	88.1	83.7	76.0	12.5
20 T 20 kN	88.1	85.9	76.0	14.0
30 T 0 kN	86.2	82.9	63.4	10.0
30 T 10 kN	86.2	81.9	63.4	10.5
30 T 15 kN	88.0	84.8	71.6	12.5
30 T 20 kN	88.0	84.8	63.4	13.0

following three stages: elastic, strain-softening, and failure, as highlighted in Fig. 18a. It should be noted that most samples exhibited an instantaneous dip of between 2 and 10 kN in their recorded shear load either at the transition point from the elastic range to the strain-softening or just after the transitioning into the strain-softening response, as demonstrated by the highlighted section of Fig. 18b. The 30-tonne rock bolt sample subject to a pretension of 15 kN was an outlier, and while it maintained a similar failure profile overall, it did not exhibit what was identified as the typical drop of 2 to 10 kN load drop, as highlighted in Fig. 18c. The transition into the strain-softening region marked the point where any deflection/deformation subjected to the sample became non-reversible. Upon inspecting the failed samples, the reduced recorded shear load could be attributed to a combination of fibreglass strand delamination, grout compressive failure, and host concrete compressive failure resulting in a momentary release of the applied load. The samples quickly recovered from the load change and continued through the strain-softening stage until they reached their peak load. The samples' peak load was represented by the greatest shear load the samples could withstand based on the resistance of the rock bolt and friction between concrete blocks prior to failure. The transition from strain-softening to failure is represented by the curve's flattening when nearing the failure limit. Once the samples achieved their failure limits, the fibres within the rock bolts failed abruptly, reducing the shear load to a residual value.

3.3.2 Pretension Profile

Each pretension axial force profile consisted of three stages: zones one, two, and three, as highlighted in Fig. 19. The first zone was represented by a linear increase in axial force, suggesting that the applied shear load was transmitted through the system with proportional losses. As the sample progressed into zone two, there was an evident overall increase in an average gradient from zone 1 to zone 2. In addition, the gradient throughout zone two gradually increased with displacement. This increase in gradient signified an increase in the transformation of shear forces to axial forces, which were then transmitted through the rock bolt. The increase in axial forces could be attributed to interface failures within the system, such that interacting zones could no longer withstand increasing loads. Some suggested interface failures could occur between the host material and grout and the grout-to-rock bolt interface. As these interfaces failed, the increasing loads were forced to transmit through the rock bolt. The final stage, as denoted by zone three, indicated the transition to total system failure. This zone was identified by a rapid drop in the gradient where an increase in displacement no longer increased in axial forces. This indicated that the fibreglass strands within the rock bolt were beginning to fail. The sample continued to progress through zone three until there was a catastrophic failure of all strands within the rock bolt.

Specific patterns were evident throughout the testing of the rock bolts with increasing pretension values. Increasing the initial set pretension subsequently increased the axial load at failure. However, this trend did not occur with each increase in pretension and was instead an overall increase from the initial 0 kN pretension sample. Figure 19b shows samples with an initially applied pretension both achieving a peak failure of 24 kN, while the sample representing the resting initial pretension only achieved a peak value of 15 kN. The data set representing the initial pretension of 15 kN was discarded from analysis due to inconsistencies during testing. In addition to the noted increase in peak axial load, there was also an observed decrease in displacement at failure. Unlike the peak load's single response to increased pretension, the displacement at failure reduced with each increase to initial pretension. Figure 19b demonstrates the reduction in failure displacement where the 0 kN pretension sample reached a displacement of 20 mm, and the 10 kN and 20 kN pretension samples achieved failure displacements of 16.5 mm and 9.5 mm, respectively. This suggests a correlation between initial pretension and failure displacement. It is noted that the samples experienced load fluctuations during

Fig. 18 **a** Example of the failure regions for 30-tonne rock bolt with ▶ a pretension of 0 kN; **b** example of the recurring reduction in shear force for the 30-tonne sample with 10 kN pretension; **c** comparison of 30-tonne rock bolt profile with and without shear force dip

curing, resulting in variability from the designed pretension setting.

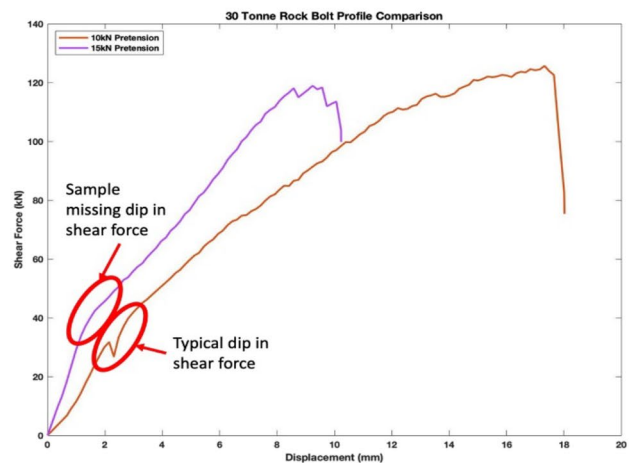### 3.3.3 Impact of Pretension on Shear Strength

The application of pretension to the 30-tonne clean shear samples had significant impact on several shear performance elements of the rock bolts including: peak shear force, failure displacement, and shear profile. The two most significant impacts to the rock bolts' performance were from the increase in pretension and were: the reduction in peak shear force and displacement as depicted by Fig. 20a. Increasing pretension resulted in an immediate reduction to the peak shear force of the tested rock bolts. However, this reduction presented as an individual phenomenon from the first pretension increase of 0–10 kN, resulting in an approximate 20% reduction of the rock bolts' peak shear capability. The increase in pretension potentially altered the confinement at each shear interface preventing the rock bolt's from transforming the shear force into an axial force. As fibreglass rock bolts can typically achieve greater peak forces axially than in shear, the presence of non-passive shear interfaces could account for the reduction in the peak shear forces for all samples subjected to pretension. Each subsequent increase in pretension presented limited new peak shear force losses. As such, the 10 kN, 15 kN, and 20 kN pretension samples all reached similar peak shear forces of between 120 and 125 kN. Unlike the one-off impact to the peak shear force, the increase in pretension resulted in incremental decreases to the samples' failure displacement with the most significant decreases occurring between the 0 kN, 10 kN, and 15 kN samples. The 0 kN sample achieved a failure displacement of more than 20 mm, while the 10 kN and 20 kN samples reached failure displacements of 17 mm and 9 mm respectively, as illustrated in Fig. 20a. This incremental reduction in shear displacement may be attributed to a tightening of the shear planes imparted through the increased axial loads caused by applying pretension. As the axial forces increased and caused artificial confinement of the shear planes, the failure limits of the elements within the systems such as the grout interface and host material increased. This resulted in reduced load losses throughout the system as previously attributed to interface failures and was further justified by the gradual elimination of the dip in shear force experienced within the strain-softening region. Figure 20b highlighted that the sample subjected to a pretension of 15 kN no longer exhibits the negative spike in shear force as experienced by the 0 kN pretension sample. Furthermore, there was a
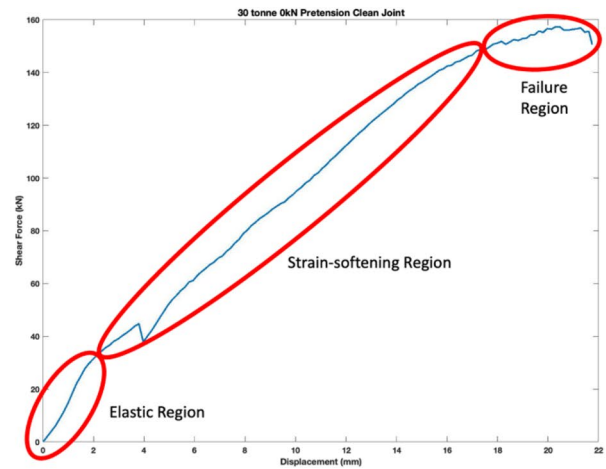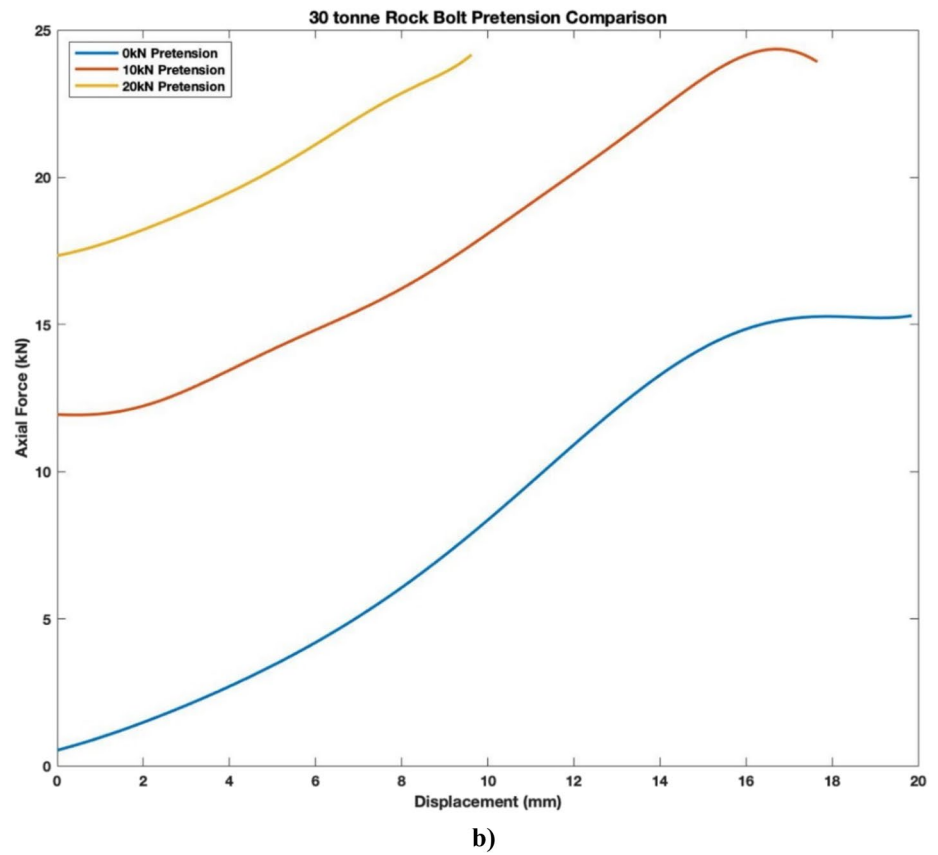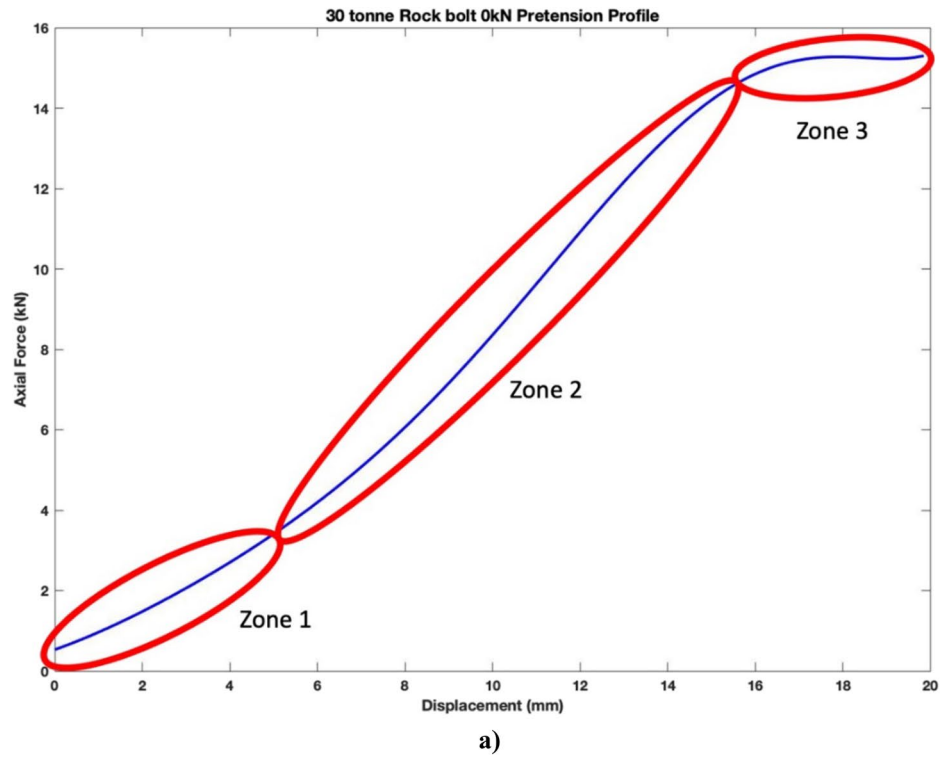

(a)
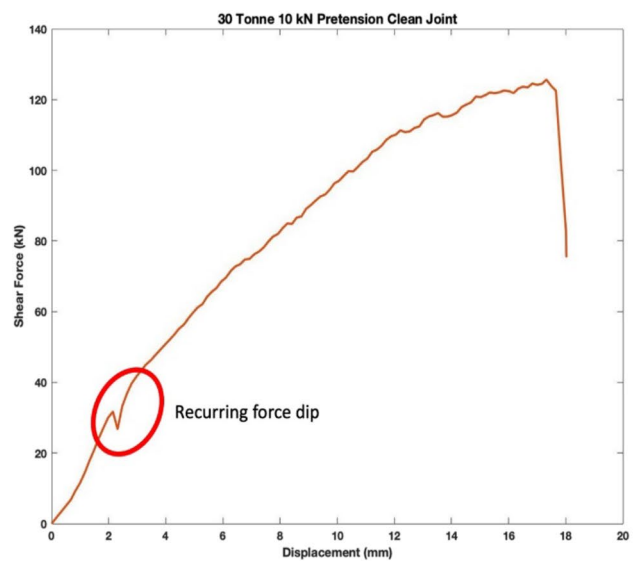
(b)

(c)

Fig. 19 **a** Illustration of the
pretension profile zones under
axial loads; **b** 30-tonne rock
bolt clean pretension profile
comparison

Fig. 20 **a** Impact of pretension on the overall shear performance of ▶ 30-tonne rock bolts with clean shear interface; **b** impact of pretension on shear force dip for 30-tonne rock bolts tested in clean shear system; **c** the effect of pretension on dip in shear force for 30-tonne rock bolts with pretensions of 0 kN, 10 kN, and 15 kN

notable reduction in spike intensity as well as displacement with each increase in pretension, until it was eliminated, as shown in Fig. 20c. Figure 20c illustrates in detail how the 10 kN pretension sample exhibited a reduced negative spike of approximately 5 kN at a displacement of 2–2.5 mm, as opposed to the 0 kN sample experiencing a negative spike of approximately 8 kN at a displacement of 3.5–4 mm. Finally, the sample subjected to 15 kN exhibited no discernible spike in shear force.

The pretension application also significantly impacted the elastic and strain-softening stages of the shear profile. The subsequent changes to pretension had an unexpected impact on the rock bolts' elastic failure response where the elastic failure force increased after the application of pretension. This increase in elastic limit occurred once and then stabilised for all subsequent increases in pretension. Additionally, there were minor incremental decreases in the displacement range of the region. Finally, the increase in pretension was observed to have a significant and proportional impact on the stiffness and strain-softening response to loading as demonstrated in Fig. 20a. The subsequent increase in slope gradient throughout the strain-softening region indicated an increase in rock bolt stiffness. While each succeeding increase in pretension increased in shear stiffness, there appeared to be no new significant impact on the peak shear performance of each rock bolt.

3.3.4 Failure Characteristics

Figure 21a, b illustrates the bending at failure for the samples subjected to 0 kN pretension and 20 kN pretension, respectively. The 20 kN pretension sample recorded a hinge point rotation of approximately 13°, an increase of 3° from the 10° recorded from the 0 kN pretension sample. This increase in angle could be attributed to an increase in confinement forces and thereby an increase to the strength of the surrounding interfaces, forcing the rock bolt to rotate around the shear plane's edge. This increase in confinement forces for the grout and host rock interfaces also resulted in less damage propagating through the rock bolt element from the shear plane as highlighted in Fig. 21a. In addition, unlike the samples with an applied pretension, the 0 kN sample had no additional axial forces applied. This lack of axial force resulted in a relaxed shear plane and interface confinements. As a result, the rock bolt experienced a lower degree of bending at the location of failure as the rock bolt forced through the surrounding material throughout the shearing
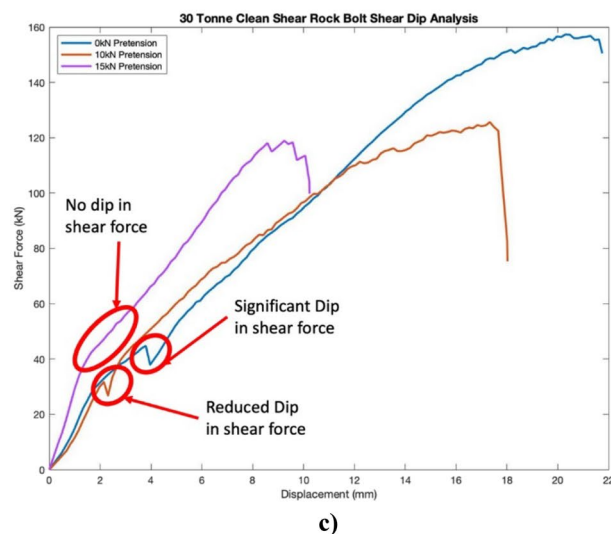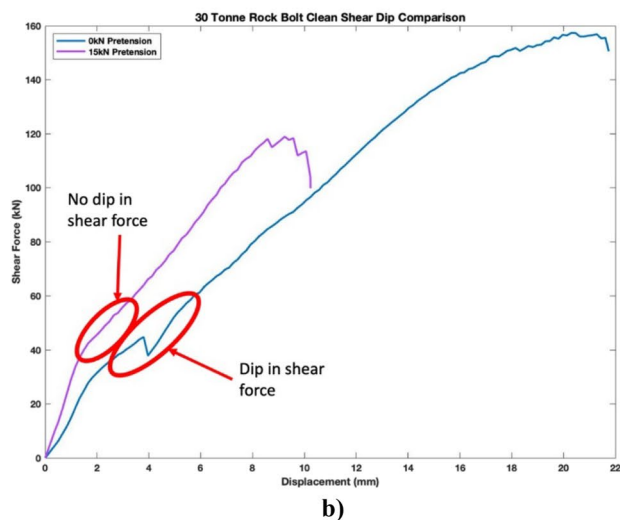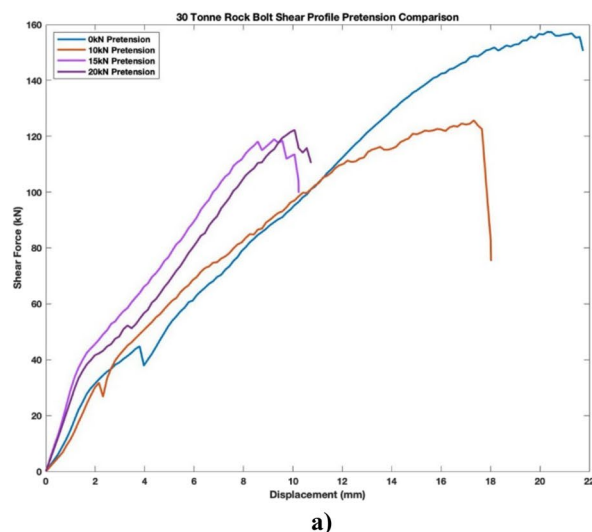
a)

b)

c)
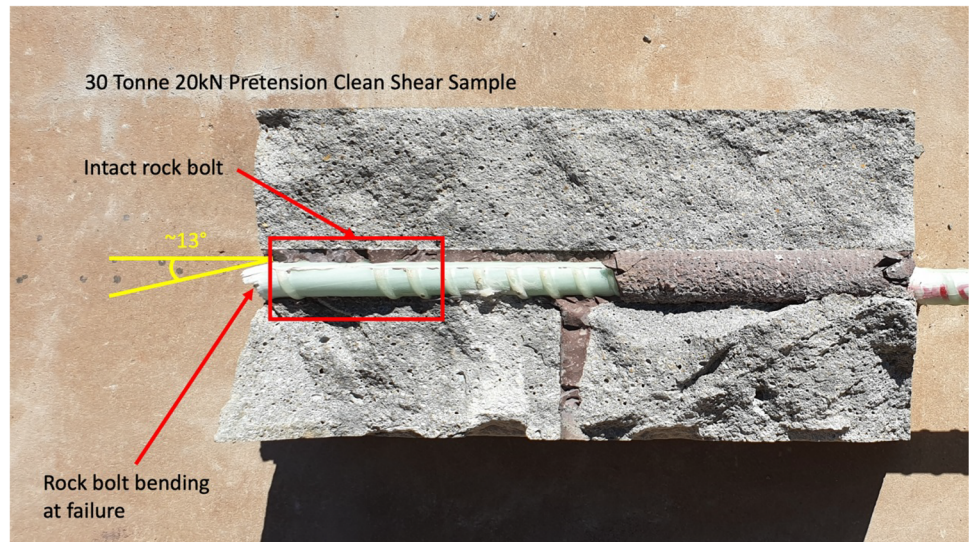
(a)
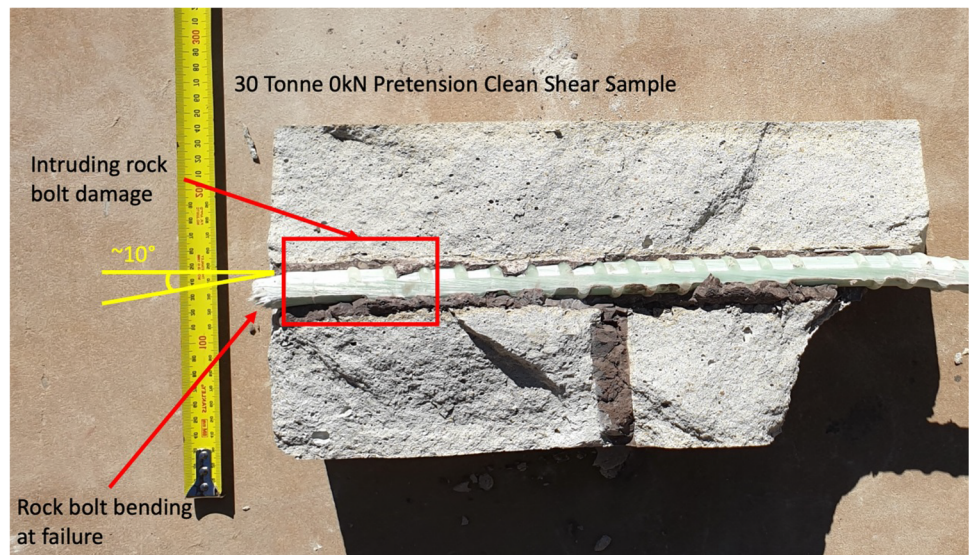
(b)

process. This caused the rock bolt to experience fractures and delamination propagating from the shear plane and extending deep within the system as highlighted in Fig. 21b.

With the increase in pretension, there appeared to be a change in the damage experienced by the surrounding material. Samples exposed to greater pretension forces caused increased damage to the shearing surface. This was due to the pretension forces creating a clamping effect across the shear planes and producing the protruding curved edge of

the hinge point, as evidenced in Fig. 21a. In addition, the curved failed edge of the rock bolt cut away a significant amount of host material from the adjacent shear plane surface. In comparison, the 0 kN samples did not share this phenomenon as the failure of the rock bolt was less aggressive, and no confining forces forced the rock bolt into the adjacent shear surface, as illustrated in Fig. 22a.

As previously outlined, the sample subjected to a pretension of 0 kN did not experience any additional confining forces like

Fig. 22 **a** Damage caused by 30-tonne rock bolt to host material with 20 kN pretension; **b** shear interface comparison 0 kN pretension and 20 kN pretension

(a)

(b)
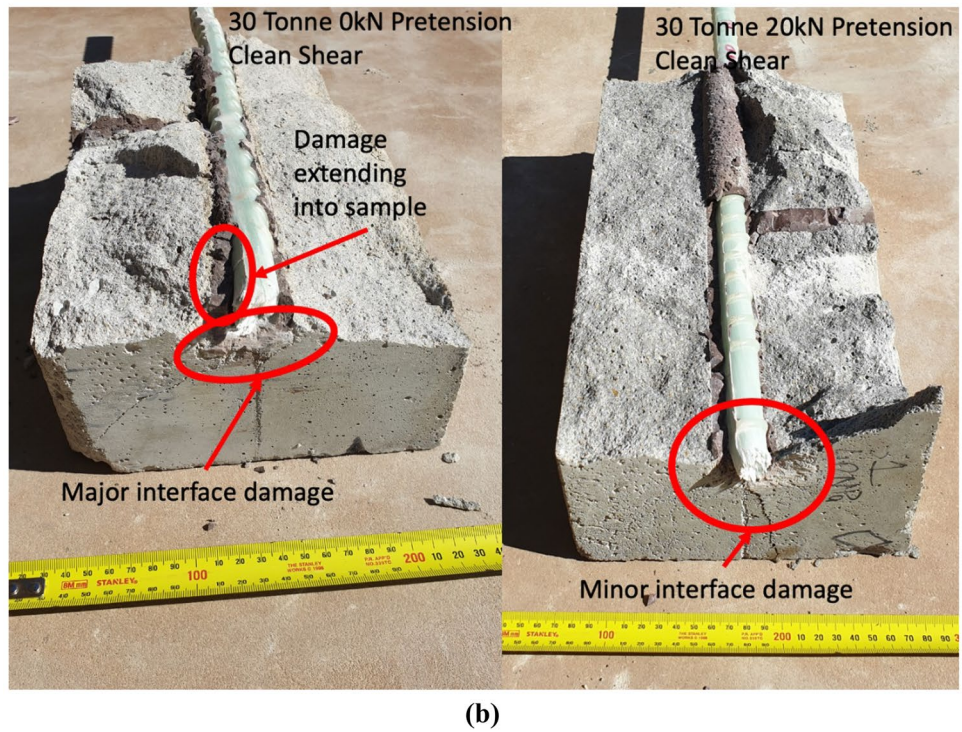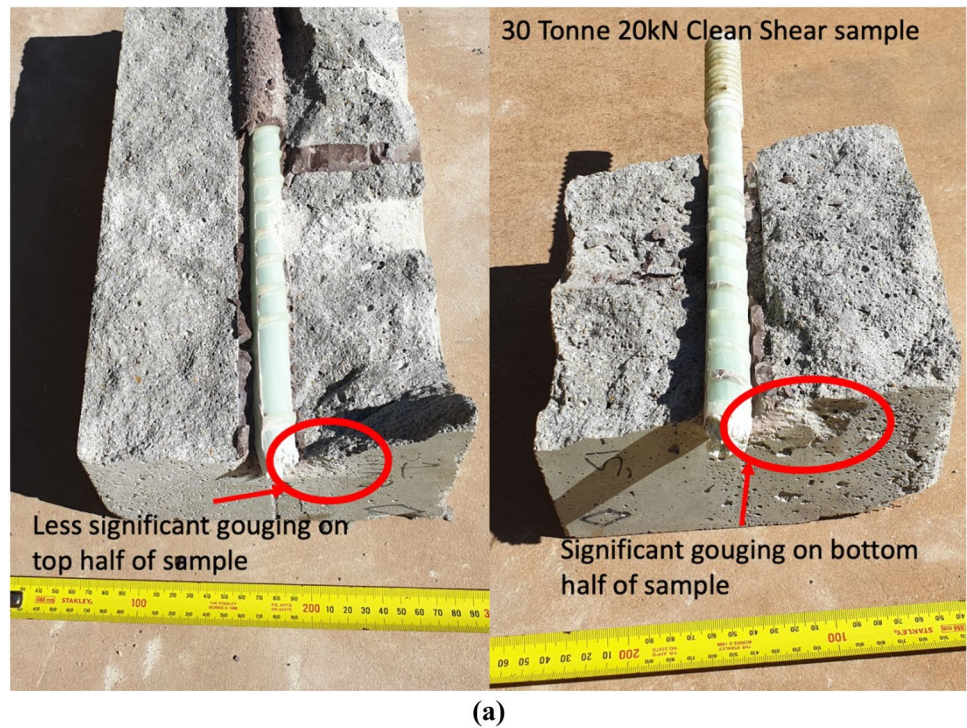
the samples with an applied pretension. This lack of additional axial forces resulted in intrinsic interface confinement pressures. Under these conditions, the introduction of shear forces along the rock bolt element caused the grout and host rock interfaces to fail, evidenced by the observed damage around the element in Fig. 22b. In contrast, samples with an applied pretension contained additional axial forces, causing an artificial increase in confinement pressures. As demonstrated in Fig. 22b, the fibreglass rock bolt was unable to overcome the increased strength of the grout and host material, resulting in significantly less damage around the rock bolt at the

Fig. 23 Shear profile comparison of 20-tonne and 30-tonne rock bolts
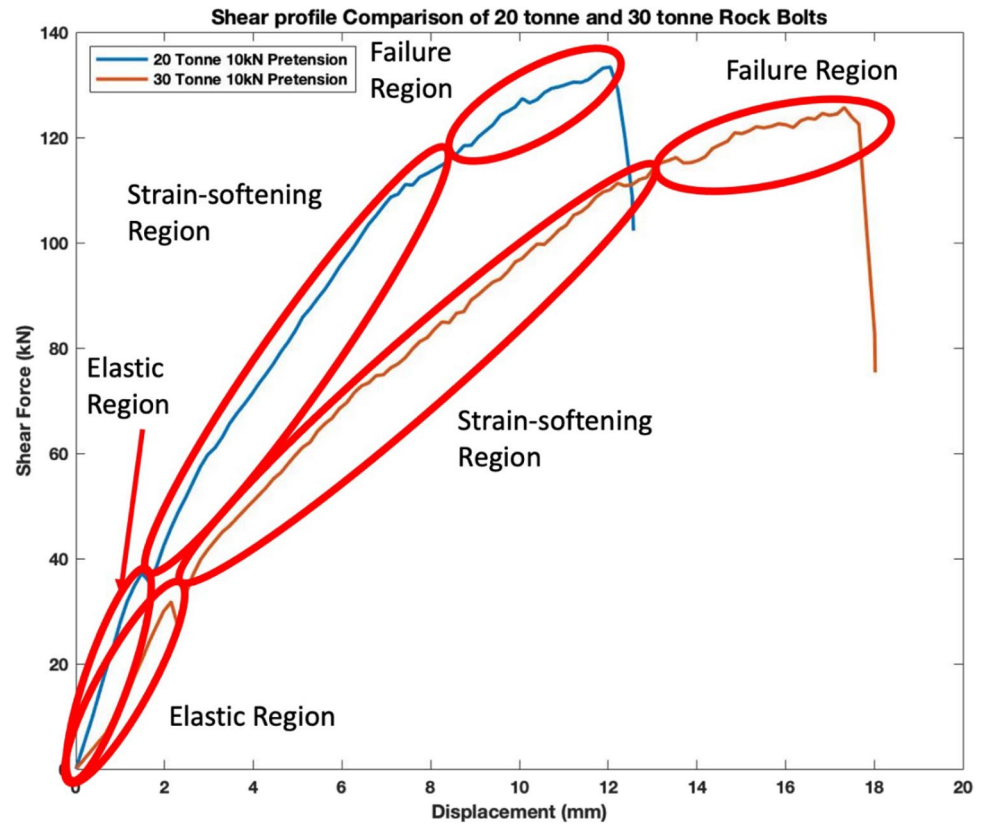
shear plane interface when compared to the sample with 0 kN pretension.

3.4 Comparison Between 20-Tonne and 30-Tonne Rock Bolts

3.4.1 Shear Behaviour Profile

The following comparative analysis outlines the similarities and differences between the shear performance of the 20-tonne and 30-tonne rock bolt types. As the results of the 20-tonne 0 kN pretension rock bolts have been discarded, the comparison has been conducted on the 10 kN samples for both 20-tonne and 30-tonne rock bolts. Comparing the elastic region across the 20-tonne and 30-tonne samples, it was evident that the elastic region observed for each bolt type was similar with respect to both plotted profile as well as their peak elastic forces. Both samples transitioned into the strain-softening stage at approximately 38 kN, as highlighted in Fig. 23a. However, these elastic regions presented with differing gradients suggesting dissimilar strain responses. The profile for the elastic region of the 20-tonne rock bolts consistently recorded a gradient of approximately 88°, somewhat steeper than the 0 kN and 10 kN pretension 30-tonne rock bolts which recorded gradients of approximately 86°, as highlighted in Table 4. This suggested that the 20-tonne

Table 5 Summary of peak forces and shear stresses of all samples

Bolt type	Peak shear force (kN)	Displacement at peak shear (mm)	Peak shear stress (GPa)
20 T0 kNC	Invalid	Invalid	Invalid
20 T10 kNC	133.3	12.1	0.42
20 T15 kNC	136.3	11.9	0.43
20 T20 kNC	133.4	8.4	0.42
30 T0 kNC	157.9	20.5	0.50
30 T10 kNC	125.5	17.3	0.40
30 T15 kNC	119.6	9.2	0.38
30 T20 kNC	122.6	10.1	0.39

rock bolts experienced a stiffer response to shear forces. The gradients observed over the elastic region of the 20-tonne samples were all greater than the gradients of the 30-tonne rock bolts. However, samples with a pretension of 15 kN and higher recorded similar results of 88.1° and 88° for the 20-tonne and 30-tonne samples, respectively. Similar to the elastic region, the strain-softening stage of the shear profile demonstrated a stiffer response to shearing for the 20-tonne samples than the 30-tonne samples, except for the 15 kN pretension samples. As highlighted in Table 4, the 20-tonne 15 kN pretension sample experienced a negligible decrease

in a gradient from the 10 kN sample, while in the same scenario, the 30-tonne sample experienced a gradient increase of 2.9°, suggesting that the 30-tonne 15 kN sample had a stiffer strain-softening region than the equivalent 20-tonne sample. Unlike the previous two stages, the final failure stage did not record an interference from changes in pretension, resulting in uniform gradients across each pretension. In the case of the 20-tonne samples, each failure zone presented with increased gradients to that of the 30-tonne samples.

Table 5 shows that the peak shear forces achieved by the 20-tonne samples subjected to pretensions of 10 kN, 15 kN, and 20 kN varied by approximately 3 kN, while the equivalent 30-tonne samples recorded a variance of approximately 6 kN. In addition to differences in stiffness, this resulted in the 30-tonne samples achieving greater displacements at failure. While the 30-tonne 0 kN pretension drastically outperformed all the other samples for peak shear, it also achieved the greatest peak displacement. However, the peak displacements achieved by the 30-tonne samples at a low pretension declined faster with each increase in pretension as opposed to the 20-tonne samples, at which point the 30-tonne 15 kN and 20 kN pretension samples matched the displacements of the 20-tonne samples. The reduced peak shear force of the 30-tonne samples could be attributed to the differences in fibre density and resin composition. Further analysis would be required to determine the correlation between shear strength and rock bolt designs optimised for tensile capacity. While there was an observed decrease in peak shear force for the 30-tonne 0 kN pretension to the 10 kN pretension, it is impossible to comment on potential similarities to the 20-tonne samples as the 0 kN sample was discarded due to inconsistencies. The 20-tonne and 30-tonne samples presented similar shear displacement trends with each increase in pretension. As identified in Table 5, each rock bolt type experienced a decrease in shear displacement when the pretension was increased. Finally, as previously shown in Table 4, the 20-tonne and 30-tonne samples exhibited similar hinge point trends as well as similar recorded values. It was observed that increasing the pretension resulted in incremental increases in bending at the hinge point post-failure. Both samples experienced hinge point bending ranging from approximately 10° to 14°. It was impossible to determine an exact value for the hinge point bending as some of the less damaged strands recovered slightly after failure; therefore, an average value was determined over the width of the failure zone.

3.4.2 Pretension Profile

As discussed earlier, both rock bolt types achieved axial pretension profiles of the same properties and both the 20-tonne and 30-tonne rock bolts' pretension profiles could be defined by three zones, as shown in Fig. 26. However, throughout the testing programme, it was identified that there were

Fig. 24 Shear profile comparison of 20-tonne and 30-tonne rock bolts
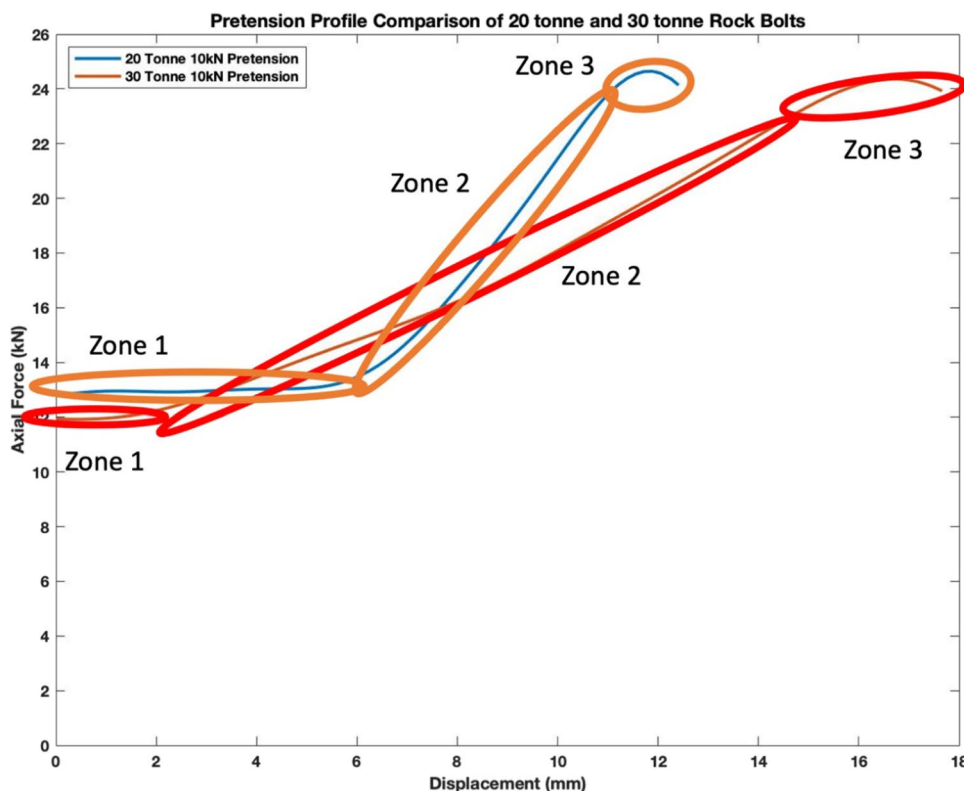
Table 6 Gradient profiles for zones 1, 2, and 3 and peak axial force for all samples

Rock Bolt	Zone (I) gradient (°)	Zone (II) gradient (°)	Zone (III) gradient (°)	Peak axial force (kN)
20 T0 kNC	–	–	–	–
20 T10 kNC	5.7	64.5	− 11.3	24.5
20 T15 kNC	5.7	45	− 5.7	20.6
20 T20 kNC	5.7	11.3	0	21.6
30 T0 kNC	26.6	1.2	11	15.7
30 T10 kNC	11.3	50.2	5.7	24.5
30 T15 kNC	11.3	38.7	0	16.7
30 T20 kNC	21.8	35	0	24.5

differences within each zone. The 20-tonne samples consistently demonstrated increased stiffnesses evident by the samples' failures at lower displacements when compared to the 30-tonne samples. The application of pretension correlated with decreased shear displacements, and as a result, both 20-tonne and 30-tonne samples exhibited a paired relationship between pretension and stiffness. This recorded stiffness difference translated to the pretension profiles. Zones one and two displayed a difference in stiffness, as evident by the comparison of the 10 kN pretension samples in Fig. 24. While zone one's gradient was consistent across the samples, there was a significant difference in its displacement range, with the 20-tonne samples exhibiting a consistently longer zone.

Zone two of the pretension profile for the 20-tonne sample recorded steeper gradients at the lower 10 kN and 15 kN pretensions when compared to the 30-tonne rock bolts as displayed in Table 6, with the exception of the 20 kN sample. The gradient difference for the 20 kN samples was potentially a result of the axial forces for the 30-tonne sample relaxing prior to testing, as evident from its lower initial pretension (consider Table 3). Despite differences in gradients, both rock bolt types experienced similar consistent reductions to the zone two gradients in relation to increased pretension. In addition to the differences with zone two, zone one displayed variations across the rock bolt types, such as differing gradients and the previously mentioned zone length. All 20-tonne samples recorded a similar gradient. Albeit lower, compared to the 30-tonne samples, throughout zone one of approximately 5.7° despite the 20-tonne sample presenting as the stiffer rock bolt. In addition, the 30-tonne rock bolt also experienced a reduction in a gradient from the 0 kN pretension sample to the 10 kN pretension sample and then later recovered the gradient following the 15 kN pretension sample. No comments could be made to compare the gradients for zone three as there was too much variation with residual forces and data system cut-off limits. However, the final peak values were successfully recorded. There appeared

to be little-to-no correlation between rock bolt type and peak axial force. The 20-tonne and 30- tonne rock bolts recorded the same peak values of 24.5 kN, suggesting that there was no correlation between the tensile and shear capabilities of the rock bolts. It is noted though that the 30-tonne sample also recorded the two lowest peak pretension results. This could be due to the system performing a more efficient shear, preventing the shear load from transforming to an axial load, potentially due to over-strengthened host concrete.

### 3.4.3 Impact of Pretension on Shear Strength

As discussed, there was an observed reduction for both peak shear force and displacement for the 30-tonne samples, which amounted to approximately 25 kN and 5 mm, respectively, when the pretension was increased to 10 kN as outlined in Tables 4 and 3 and further illustrated in Fig. 25a. The reduction of shear force experienced by the 30-tonne sample resulted in the subsequent samples achieving similar results to the equivalent 20-tonne samples. Figure 25a demonstrates that the new peak shear force of the 30-tonne sample now closely resembled the shear force of the 20-tonne sample with a variation of only 8 kN. The observed failure displacements did not agree despite the similar shear force values. The 30-tonne 10 kN pretension sample was displaced an additional 7.6 mm at the moment of failure when compared to the 20-tonne equivalent sample. The failure displacement for the 20-tonne sample was considerably less than the 30-tonne sample, suggesting that the 20-tonne sample displayed a stiffer response to shearing than the 30-tonne sample. However, the reverse could be said when comparing samples transitioning to 15 kN pretension. Indeed, increasing the pretension further to 15 kN resulted in a continued trend of reduction in shear force and displacement for the 30-tonne sample. As a result, the 30-tonne sample with a pretension of 15 kN failed with a shear displacement of 1 mm less than the 20-tonne sample of the same pretension, therefore presenting as the stiffer rock bolt option. This trend, however, did not continue as the two rock bolt types displayed two opposing peak displacement responses to increased pretension. In contrast, the 30-tonne samples demonstrated significant reductions in the peak displacement, and this effect reduced with each increase in pretension, resulting in very little variation between the peak displacements of the 15 kN and 20 kN samples, as illustrated in Fig. 25b. In contrast, the reverse observation was made for the peak displacement of the 20-tonne rock bolts, where the initial change of pretension from 10 to 15 kN showed a minor change of less than 0.5 mm. However, the change from 15 to 20 kN pretension resulted in a much greater decrease of 3.5 mm in displacement for the 20-tonne samples, as shown in Fig. 25b. The 20-tonne rock bolt with a
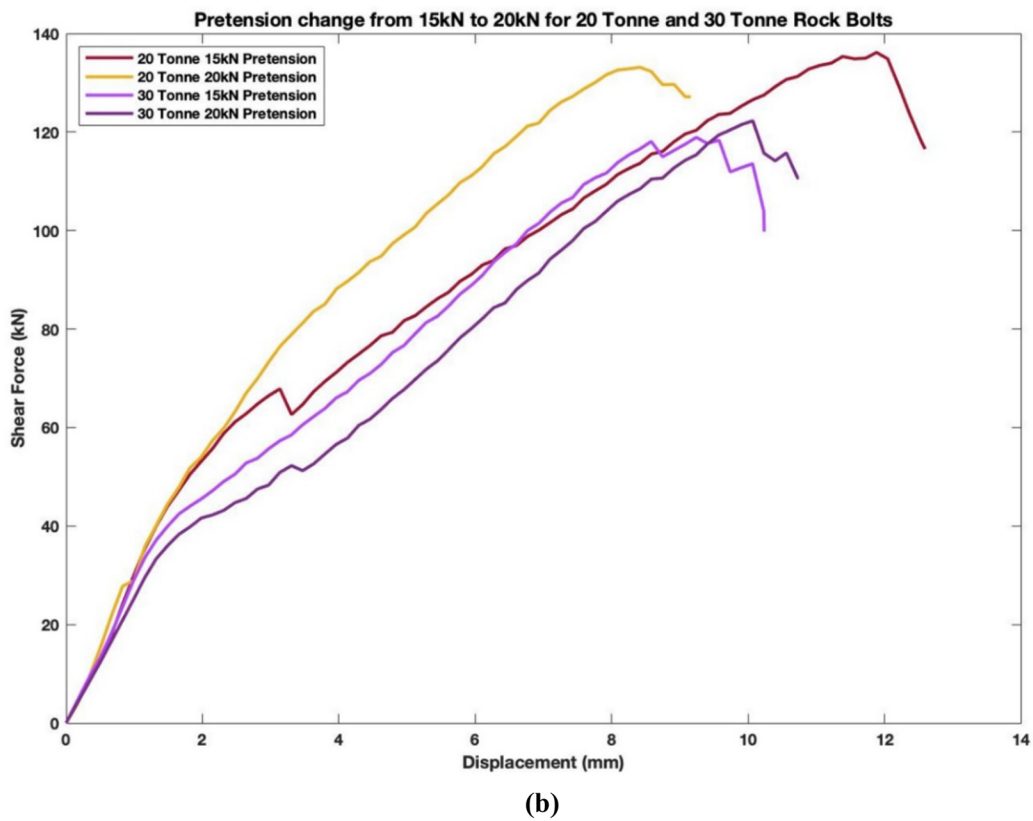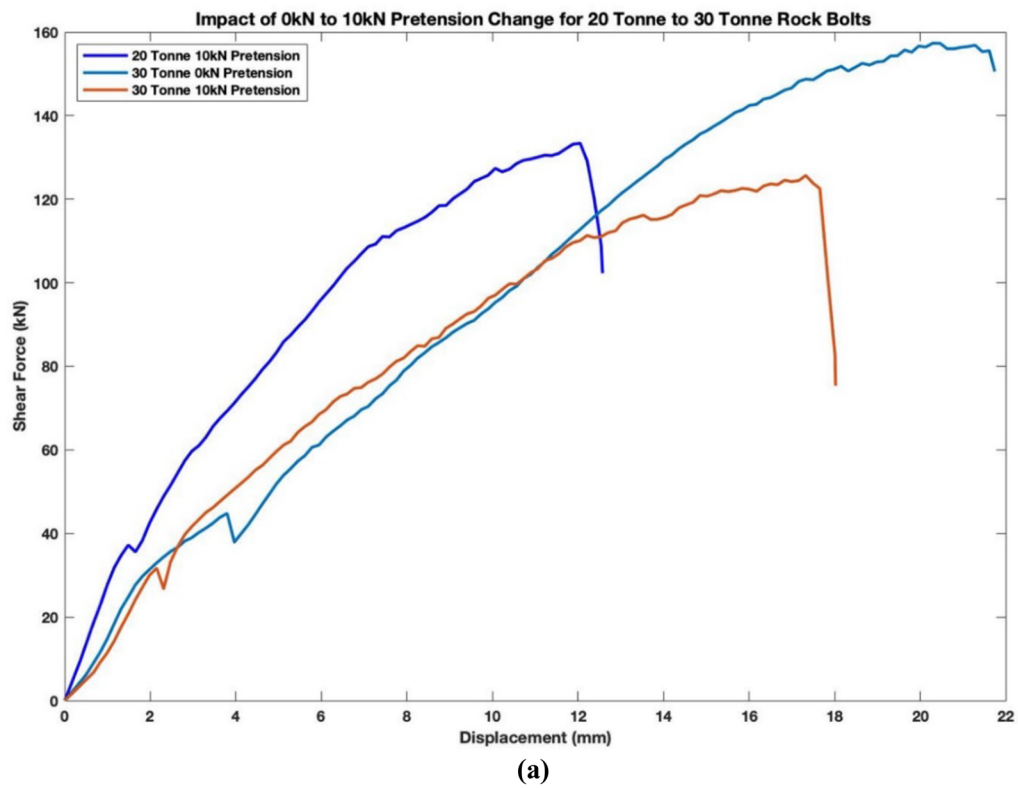
Fig. 25 **a** Influence of pretension increase from 0 to 10 kN on shear force for 20-tonne and 30-tonne rock bolts; **b** influence of pretension increase from 15 to 20 kN on shear force for 20-tonne and 30-tonne rock bolts

Fig. 26 a Comparing rock bolt structural damage for 20-tonne and 30-tonne rock bolts with 20 kN pretension; **b** representation of shear plane damage for 20-tonne and 30-tonne rock bolts
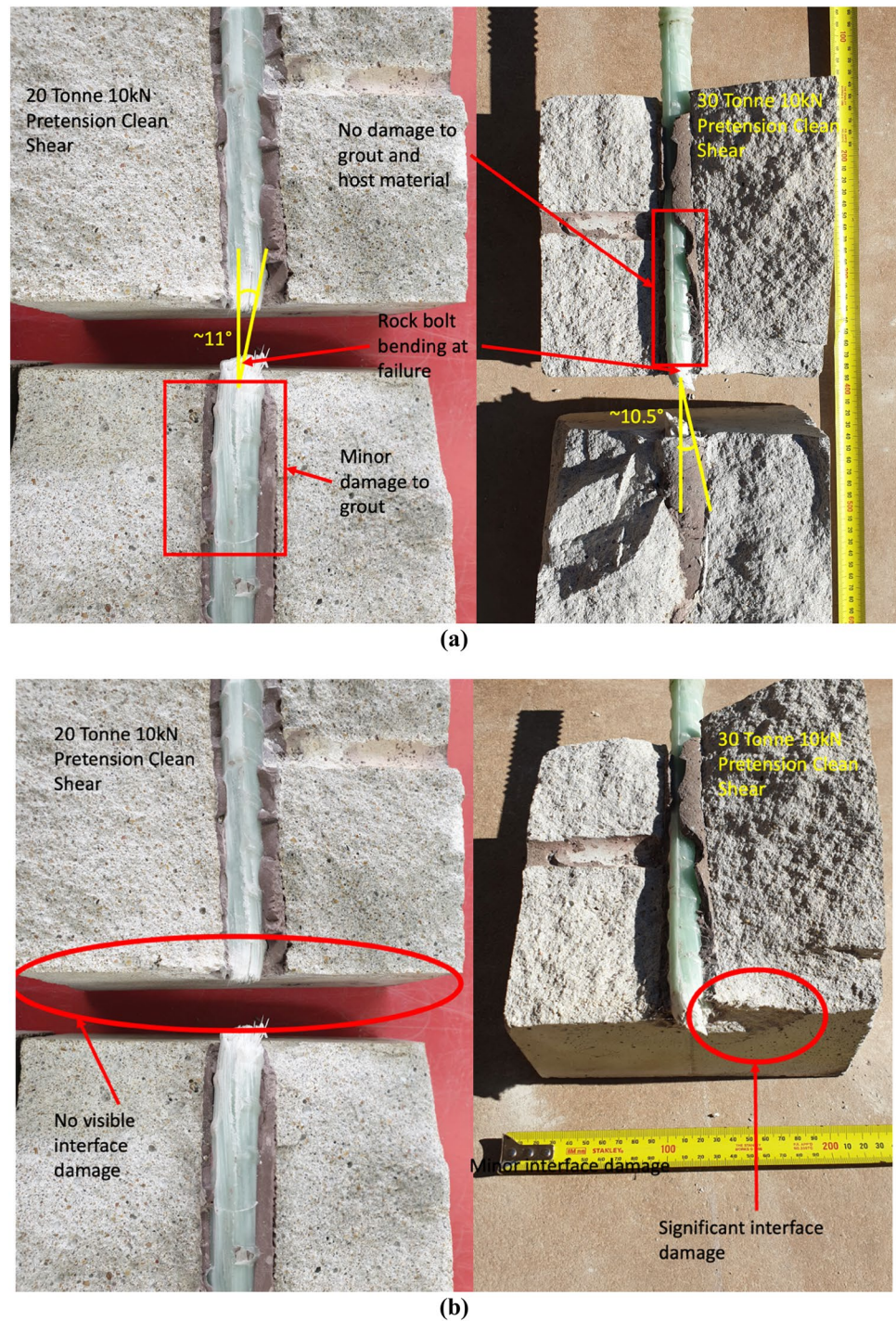
pretension of 20 kN was again the stiffer system compared to the 30-tonne rock bolt of the same pretension.

For all samples, the shear force dip was observed to have occurred either at the end of the elastic region or just following the beginning of the strain-softening region, suggesting that this phenomenon was a result of either the system as a whole or an intrinsic fibreglass response. Further testing would be required to determine the root cause. Overall, it

was evident that the application of pretension had a positive impact on the reduction of the intensity of the dip, and with a large enough pretension, the dip could be eliminated altogether. It was observed that each increase in pretension had a greater impact in reducing the dip in the 30-tonne samples than the 20-tonne samples. A pretension of 15 kN was required by the 30-tonne samples for the dip to be eliminated. However, the 20-tonne sample still presented

remnants of the phenomenon with a pretension of 20 kN, as demonstrated in Fig. 25b.

3.4.4 Failure Characteristics

Sections 3.2.4 and 3.3.4 provide a detailed analysis of the failure characteristic of each rock bolt and highlight three key components of failure: the hinge point, the rock bolt structural damage, and the shear surface damage. In the 10 kN pretension samples it was evident that the 20-tonne and 30-tonne rock bolts had similar properties when analysing the hinge point. Both samples achieved similar failure angles with a difference of 0.5° as demonstrated in Fig. 26a. However, this was the only similarity for the 10 kN pretension samples. When assessing the structural damage within the rock bolts, the 20-tonne sample displayed evidence of fractures propagating deeper into the sample. In contrast, the 30-tonne rock bolt displayed no internal fractures, as highlighted in Fig. 26a. Figure 26b shows that the 30-tonne rock bolts displayed the ability to damage the shear plane surface when there was an applied pretension of greater than 0 kN. The damage depicted in Fig. 26b resulted from the 30-tonne rock bolt dragging across the surface. However, it can be seen that the 20-tonne rock bolt with the same 10 kN pretension did not share this characteristic, and as a result, no damage was observed on the shear plane. The 20-tonne rock bolt exhibited signs of damage to the grout layer surrounding the rock bolt, unlike the 30-tonne sample, as shown in Fig. 26a.

Like the 10 kN pretension samples, both the 20-tonne and 30-tonne rock bolts, subjected to 20 kN pretension, performed similarly when investigating the bending at the hinge point. However, the difference in recorded angles deviated from the 0.5° recorded for the 10 kN samples to 1° for the 20 kN samples. While the deviation increased, the rock bolts performed similarly to the trends outlined in Table 4. Unlike the 10 kN pretension samples, the 20 kN pretension samples displayed similar structural performance and neither the 20-tonne or 30-tonne rock bolt displayed any propagating fractures from the zone of damage. Additionally, neither of the rock bolts displayed damage to the grout and host material interfaces due to the increased confinement due to the pretension.

Despite the 30-tonne samples causing damage to the shear plane through gouging across all the tested pretensions during shearing, none of the 20-tonne samples presented damage to the shear plane as a direct result of the rock bolt. Figure 27a highlights that even when the 20-tonne rock bolt is installed with the highest pretension setting of 20 kN, no damage was sustained to the shearing surface. In contrast, Fig. 27b highlights the damage sustained by the shear plane due to the 30-tonne rock bolt.


(a)

(b)
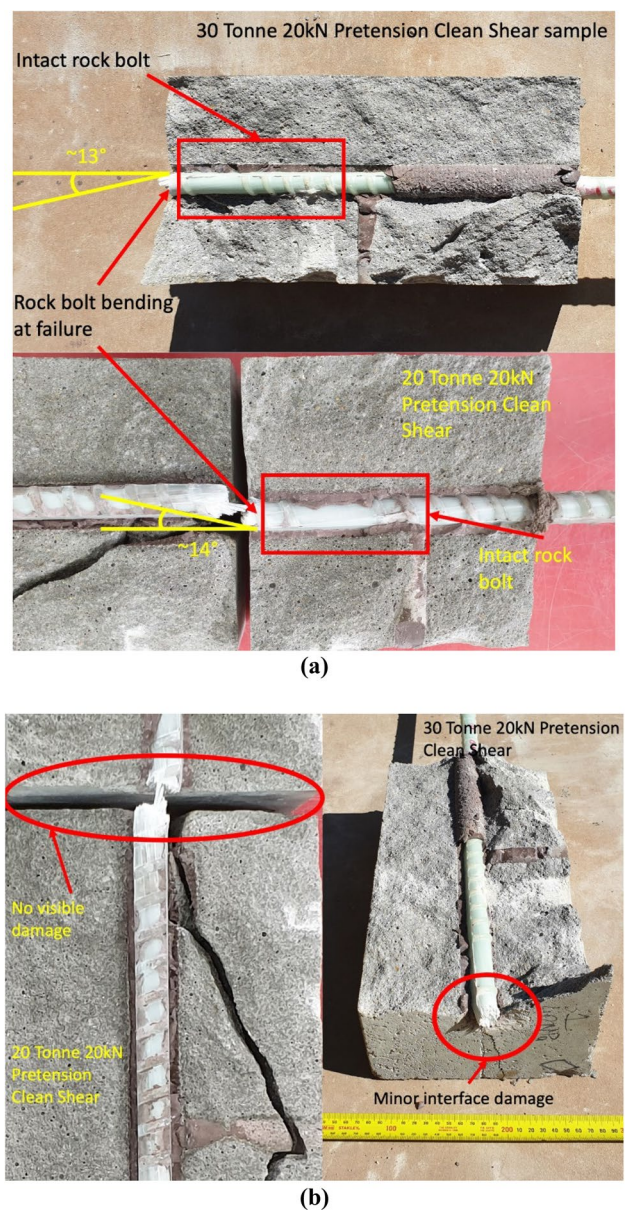
Fig. 27 a Comparing rock bolt structural damage for 20-tonne and 30-tonne rock bolts with 20 kN pretension; **b** representation of shear plane damage for 20-tonne and 30-tonne rock bolts

3.5 Understanding the Behaviour of Fibreglass Rock Bolts

3.5.1 Shear Behaviour Profile

The 20-tonne and 30-tonne rock bolts tested using the single shear testing method demonstrated comparable shear profiles containing the three regions as shown in Fig. 28. The first region was the initial linear stage of the profile and was classified as the elastic region due to its apparent elastic response; therefore, any failure occurring during

**Fig. 28** Stages of the single shear profile for 20-tonne and 30-tonne rock bolts
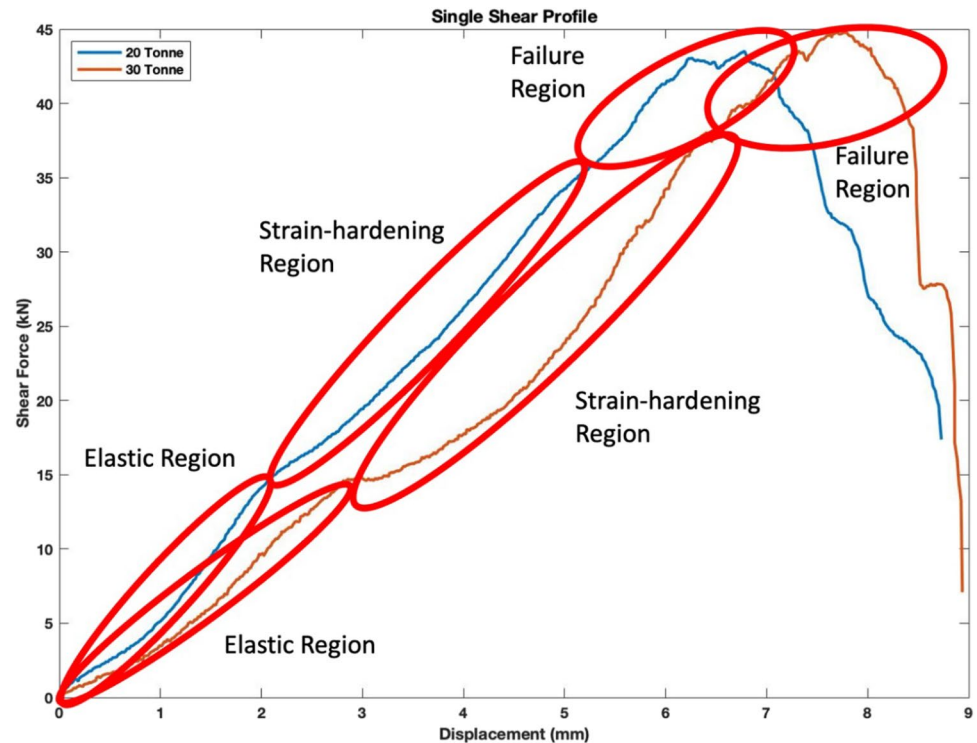
stage one was reversible and caused no damage to the rock bolt. A positive nonlinear shear force increase identified the second stage with the increased displacement. This characteristic suggested the rock bolt experienced a form of hardening, and therefore, the region was aptly named the strain-hardening region. Strain-hardening was suspected to occur due to the single shear apparatus providing increasing axial confinement. Throughout the shearing action of the guillotine, the rock bolts' annulus decreased as the two halves of the shearing apparatus slid past each other as the displacement increased. Therefore, the rock bolt was forced to occupy a decreasing area at the shear face. This, in turn, provided increasing shear force transfer efficiency throughout the rock's cross-section as forces were unable to dissipate through resin failure. This resulted in the observed increase in recorded shear force. The final region was identified as the failure region due to the reducing shear force response to displacement occurring through a mixture of significant instantaneous reductions in shear force as well as gradual declines. It was evident in both cases that the reducing shear force was a result of the fibres and resin structure failing and leading to complete rock bolt rupture. Both rock bolt samples performed similarly achieving similar peak shear forces and displacements. The main difference between the rock bolt types was the failure displacement and strain throughout each region. During the elastic and strain-hardening portions of the shear profile, the 20-tonne rock bolt demonstrated a stiffer response to shear, as illustrated in Fig. 28. The limits of each stage across the rock bolt types were similar;

however, the 20-tonne sample reached its peak shear force at lower displacements compared to that of the 30-tonne rock bolt. This resulted in the 20-tonne sample beginning the failure stage 1 mm earlier than the 30-tonne sample. Despite achieving similar peak shear force values at differing displacements, rock bolts achieved ultimate failure within 0.2 mm of each other. The post-failure response of the 20-tonne rock bolt was drawn out over a longer period as evident by smaller decreases in the recorded shear forces. In contrast, the 30-tonne rock bolt demonstrated a greater number of significant and instantaneous decreases in the shear force.

Throughout the completion of the double shear analysis, it became obvious that several key shearing behaviours experienced were also evident during the single shear tests, such as the shear profile and the difference in performance due to rock bolt type. The single shear and double shear testing methods both identified a shear profile consisting of three stages, including the elastic region, a strain failure response region, and, finally, the failure region, demonstrated in Fig. 29. While the second stages identified opposite strain responses, such that the double shear samples exhibited a strain-softening behaviour and, therefore, opposite to the strain-hardening behaviour of the single shear test. It was concluded that the strain response region was an intrinsic property of the rock bolt, whereas the type of strain response experienced was a function of the testing system. The double shear and single shear testing methods confirmed that the tensile capacity of the rock bolts had a limited impact

Fig. 29 Shear behaviour of 30-tonne rock bolts outlining double shear and single shear stages
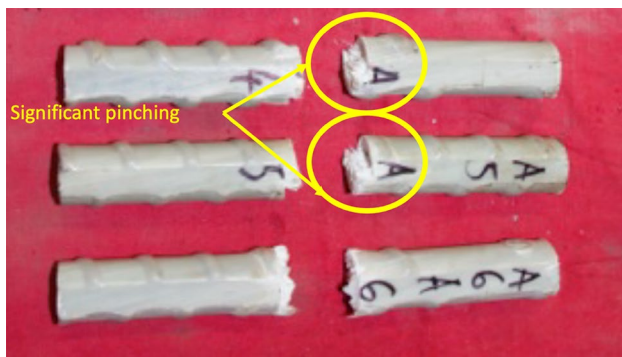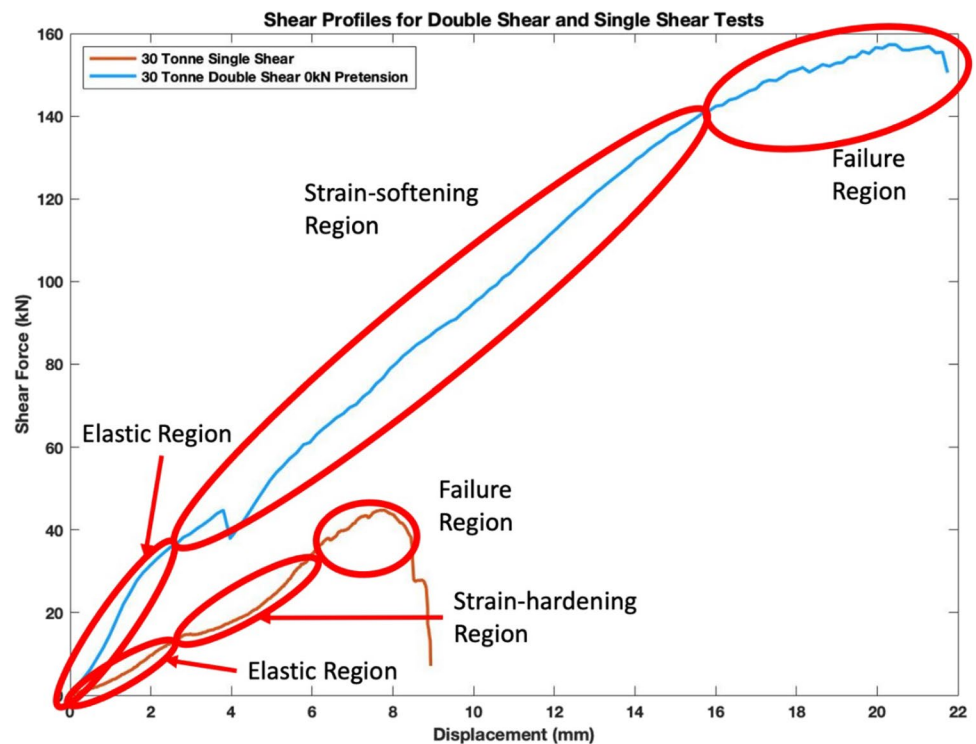
Fig. 30 Shear behaviour of 30-tonne rock bolts outlining double shear and single shear stages

on their overall shear performance. The changes in confinement pressures because of the applied pretension were an influencing factor for the performance differences between the rock bolt types impacting the strain response of the rock bolts. Also, increasing the pretension facilitated the efficient transfer of shear forces directly to the rock bolt. This resulted in the decrease of the failure shear force and peak displacement of each rock bolt and with each increase in pretension the rock bolt's performance stabilised across the rock bolt types. The 20-tonne and 30-tonne samples exhibited increasingly similar shear properties to that of the single shear samples.

3.5.2 Single Shear Failure Characteristics

The single shear samples were analysed post-failure to determine the presence of outlying physical characteristics. It should be noted that some assumptions were made regarding the physical influence the single shear apparatus had on the rock bolts. It was assumed that during the shearing process, the lateral confinement subjected to the rock bolt at the shear plane increased due to the reducing volume within the chamber. At the beginning of the shearing process, the shear plane was debris free, and no lateral confinement was present, resulting in the clean shearing of the fibreglass strands, as illustrated by the flat edges of the sheared surface in Fig. 30.

As shearing neared completion, the confinement at the shear plane increased, providing additional forces on the fibreglass rock bolt and forced the resin and fibreglass strands to crumble. The crumbling effect can be observed in Fig. 30 across the centreline of the highlighted rock bolts. This progressed until the shear failure force was achieved and the sample split in two. It was observed that the damage caused by shearing was limited to within 5 mm of the shear face. In contrast to the damage displayed by the 20-tonne and 30-tonne double shear tests outlined in Sects. 3.2.4 and 3.3.4, the single shear samples did not present any additional crack propagation from the shear face. Finally, the failure faces of the single shear samples were perpendicular to the orientation of the rock bolt, as shown in Fig. 30. This shearing behaviour was in contrast to the samples tested using the

double shear test system, which exhibited varying degrees of rotation.

4 Conclusion

In this paper, the shear performance of the fibreglass rock bolts with clean shear interfaces has been investigated by conducting the clean joint test scheme. For this purpose, the double shear testing apparatus was modified to address the issues and shortcomings of the established testing methodology. The modified testing apparatus provided new insights into the shear behaviour properties of fibreglass rock bolts while also minimising the limitations encountered by the previous studies. Also, the test scheme and equipment were designed to allow for simultaneously testing additional system parameters while subjecting shear forces. This allowed the testing apparatus to monitor the rock bolts' axial response to shearing and examine the influence changes to the system's conditions can have on the overall performance of the rock bolts. Experiments were also subjected to various system properties to ensure a comprehensive study. These properties included fibreglass rock bolts of 20-tonne and 30-tonne tensile capacities and pretensions of 0 kN, 10 kN, 15 kN, and 20 kN. Great care was taken during sample preparation to ensure sample uniformity; however, achieving the specified pretensions proved to be a difficult task. Variability in the rock bolts' quality resulted in several discarded bolts during assembly and one discarded test sample. Despite the challenges introduced by the quality of the rock bolts, several shear behaviour characteristics were identified. First, the clean shear test scheme categorised the shear profile as elastic, strain-softening, and failure regions. While it was found that all clean joint samples experienced these regions, the increasing pretension caused a reduction in the displacement and shear range of some of the rock bolts. The increase in applied pretension also resulted in increased shear profile smoothing. However, pretension had little-to-no impact on the 20-tonne rock bolts' shear failure force. Instead, the tensile load rating influenced the systems' strain response, whereby the 30-tonne samples experienced failure at more significant displacements. Finally, clean joint samples subjected to increased pretension forces experienced a more efficient transfer of shear forces through the system and to the rock bolt, resulting in less damage propagating away from the rock bolt at the shear interface.

Declarations

References

Aziz N, Pratt D, Williamas R (2003) Double shear testing of bolts. In: Aziz N (ed) Coal operators' conference. The University of Wollongong, Wollongong

Aziz N, Craig P, Nemcik J, Hai FI (2013) Rock bolt corrosion—an experimental study. In: Aziz N (ed) Coal operators' conference. The University of Wollongong, Wollongong

Aziz N, Craig P, Mirzaghorbanali A, Rasekh H, Nemcik J, Li X (2015a) Behaviour of cable bolts in shear; experimental study and mathematical modelling. In: Aziz N (ed) 15th coal operators' conference. University of Wollongong, Wollongong

Aziz N, Mirzaghorbanali A, Nemcik J, Rasekh H, Li X (2016) A follow up to study the behaviour of cable bolts in shear: experimental study and mathematical modelling. In: Aziz N (ed) 16th coal operators' conference. University of Wollongong, Wollongong

Aziz N, Rink O, Rasekh H, Hawkins E, Mirzaghorbanali A, Yang G, Khaleghparast S, Mills K, Jan N, Li X (2017) Single shear testing of various cable bolts used in Australian mines. In: Aziz N (ed) 17th coal operators' conference. University of Wollongong, Wollongong

Aziz N, Gilbert D, Nemcik J, Mirzaghorbanali A, Burton R (2015b) The Strength properties of Fiber glass and other polymer based Dowels for Strata Reinforcement in Coal mines. In: Third Australian Ground Control in Mining Conference. Ausimm, Sydney

BS 7861 (2009) Strata reinforcement support system components used in coal mines—part 1: specification for rockbolting and part 2: Specification for Flexible systems for roof reinforcement.: BSI

Chang X, Wang G, Liang Z, Yang J, Tang C (2017) Study on grout cracking and interface debonding of rockbolt grouted system. Constr Build Mater 135:665–673

Clifford B, Kent L, Altounyan P, Bigby D (2001) Systems used in coal mining development in long tendon reinforcement. In: 20th international conference on ground control in mining. West Virginia, USA

DSI-UNDERGROUND (2021) Rock Bolts—FRP [Online]. Online: DSI UNDERGROUND. https://www.dsiunderground.com.au/products/mining/rock-bolts/

Forbes B, Vlachopoulos N, Diederichs MS, Aubertin J (2020) Augmenting the in-situ rock bolt pull test with distributed optical fiber strain sensing. Int J Rock Mech Min Sci 126:104202

Frketic J, Dickens T, Ramakrishnan S (2017) Automated manufacturing and processing of fiber-reinforced polymer (FRP) composites: an additive review of contemporary and modern techniques for advanced materials manufacturing. Addit Manuf 14:69–86

Gilbert D, Mirzaghorbanali A, Li X, Rasekh H, Aziz N, Nemcik J (2015) Strength properties of fibre glass dowels used for strata reinforcement in coal mines. In: Aziz N (ed) Coal operators' conference. University of Wollongong, Wollongong

Hartman W, Hebblewhite B (2003) Understanding the performance of rock reinforcement elements under shear loading though laboratory testing—a 30-year History. 1st AGCM Conference

Hassell R, Villaescusa E, Thompson A, Kinsella B (2004) Corrosion assessment of ground support systems. In: Villaescusa E, Potvin Y (eds) Ground Support in mining and underground construction. Taylor and Francis Group, London

Jahangir E, Blanco-Martin L, Hadj-Hassen F, Tijani M (2021) Development and application of an interface constitutive model for fully grouted rock-bolts and cable-bolts. J Rock Mech Geotech Eng 13:811–819

Jennmar (2021) 32MM Fibreglass Torque Tension Bolt. Online: Jennmar Australia

Li X, Aziz N, Mirzaghorbanali A, Nemcik J (2016) Behavior of fiber glass bolts, rock bolts and cable bolts in shear. Rock Mech Rock Eng 49:2723–2735

Li F, Quan X, Jia Y, Wang B, Zhang G, Chen S (2017a) The experimental study of the temperature effect on the interfacial properties of fully grouted rock Bolt. Appl Sci 7:327

Li X, Aziz N, Mirzaghorbanali A, Nemcik J (2017b) Comparison of the shear test results of a cable bolt on three laboratory test apparatuses. Tunn Undergr Space Technol 61:82–89

Maranan G, Manalo A, Karunasena K, Benmokrane B (2015) Bond stress-slip behavior: case of GFRP bars in geopolymer concrete. J Mater Civ Eng 27:04014116

MEGA-BOLT (2021) High capacity strata support products and systems for underground mining. Online: MEGA BOLT.

Minova (2021) Steel and Fibreglass. Online: MINOVA.

Mirzaghorbanali A, Rasekh H, Aziz N, Yang G, Khaleghparast S, Nemcik J (2017) Shear strength properties of cable bolts using a new double shear instrument, experimental study, and numerical simulation. Tunn Undergr Space Technol 70:240–253

Nemcik J, Gale WJ, Fabjanczyk MW (2006) Methods of interpreting ground stress based on underground stress measurements and numerical modelling. In: Aziz N (ed) Coal operators' conference. University of Wollongong, Wollongong

Rajapakse R (2016) 33—Rock bolts, dowels, and cable bolts. In: Rajapakse R (ed) Geotechnical engineering calculations and rules of thumb, 2nd edn. Butterworth-Heinemann, Oxford

Reserve Bank of Australia (2020) Snapshot Comparison [Online]. Webpage: Reserve Bank of Australia

Spearing A, Mondal K, Bylapudi G (2010) The corrosion of rock anchors in US coal mines. In: SME, Annual Meeting. Phoenix: SME

Thenevin I, Blanco-Martin L, Hadj-Hassen F, Schleifer J, Lubosik Z, Wrana A (2017) Laboratory pull-out tests on fully grouted rock bolts and cable bolts: Results and lessons learned. J Rock Mech Geotech Eng 9:843–855

Thompson A, Villaescusa E (2014) Case studies of rock reinforcement components and systems testing. Rock Mech Rock Eng 47:1589–1602

Waclawik P, Ram S, Kumar A, Kukutsch R, Mirek A (2019) Field and simulation study for rock bolt loading characteristics under high stress conditions. In: Aziz N (ed) 19th coal operators' conference. University of Wollongong, Wollongong

Windsor CR (1997) Rock reinforcement systems. Int J Rock Mech Min Sci 34:919–951

Windsor C, Thompson A (1992) Reinforcement design for jointed rock masses. In: Proceedings of the 33rd US symposium on rock mechanics